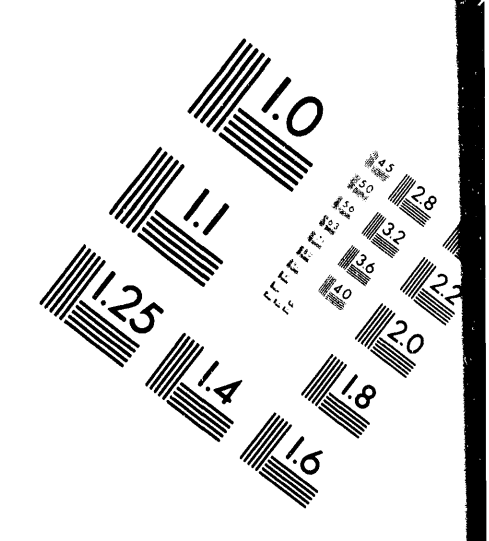
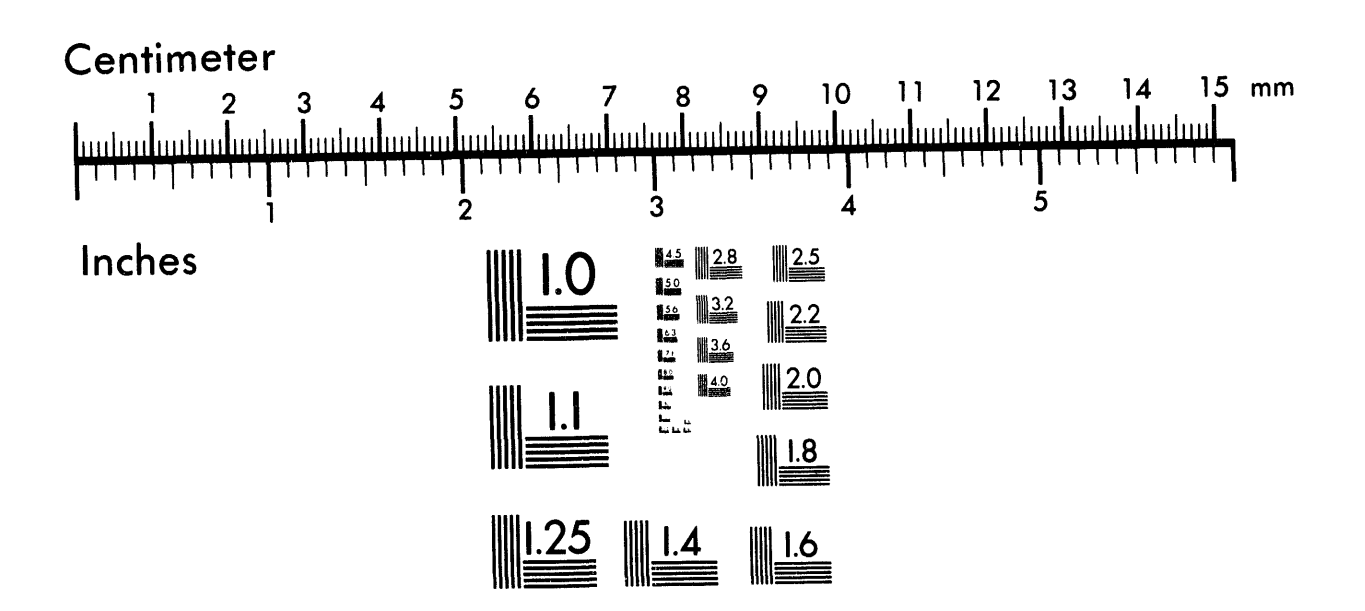


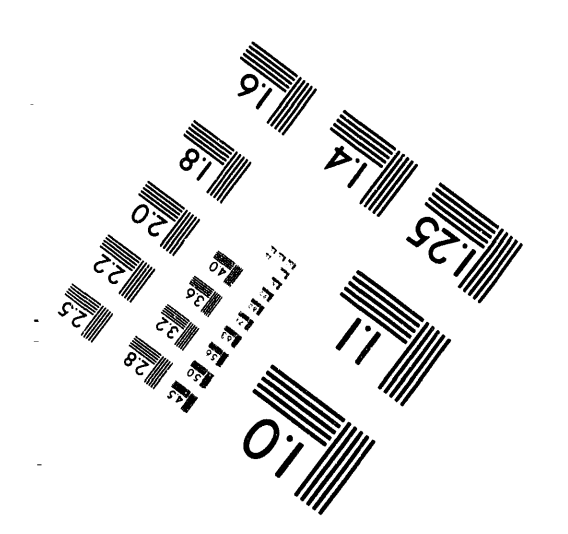


Association for Information and Image Management

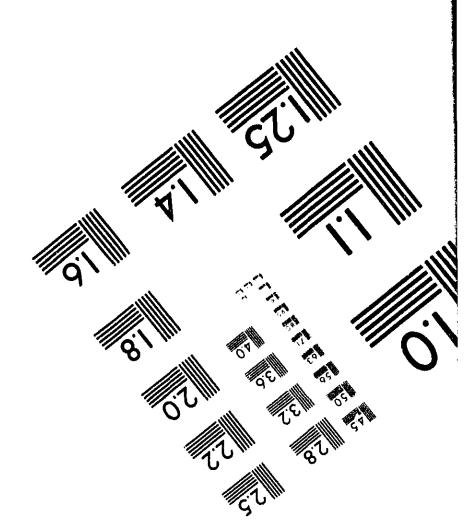
1100 Wayne Avenue, Suite 1100 Silver Spring, Maryland 20910 301/587-8202







MANUFACTURED TO AIIM STANDARDS
BY APPLIED IMAGE, INC.

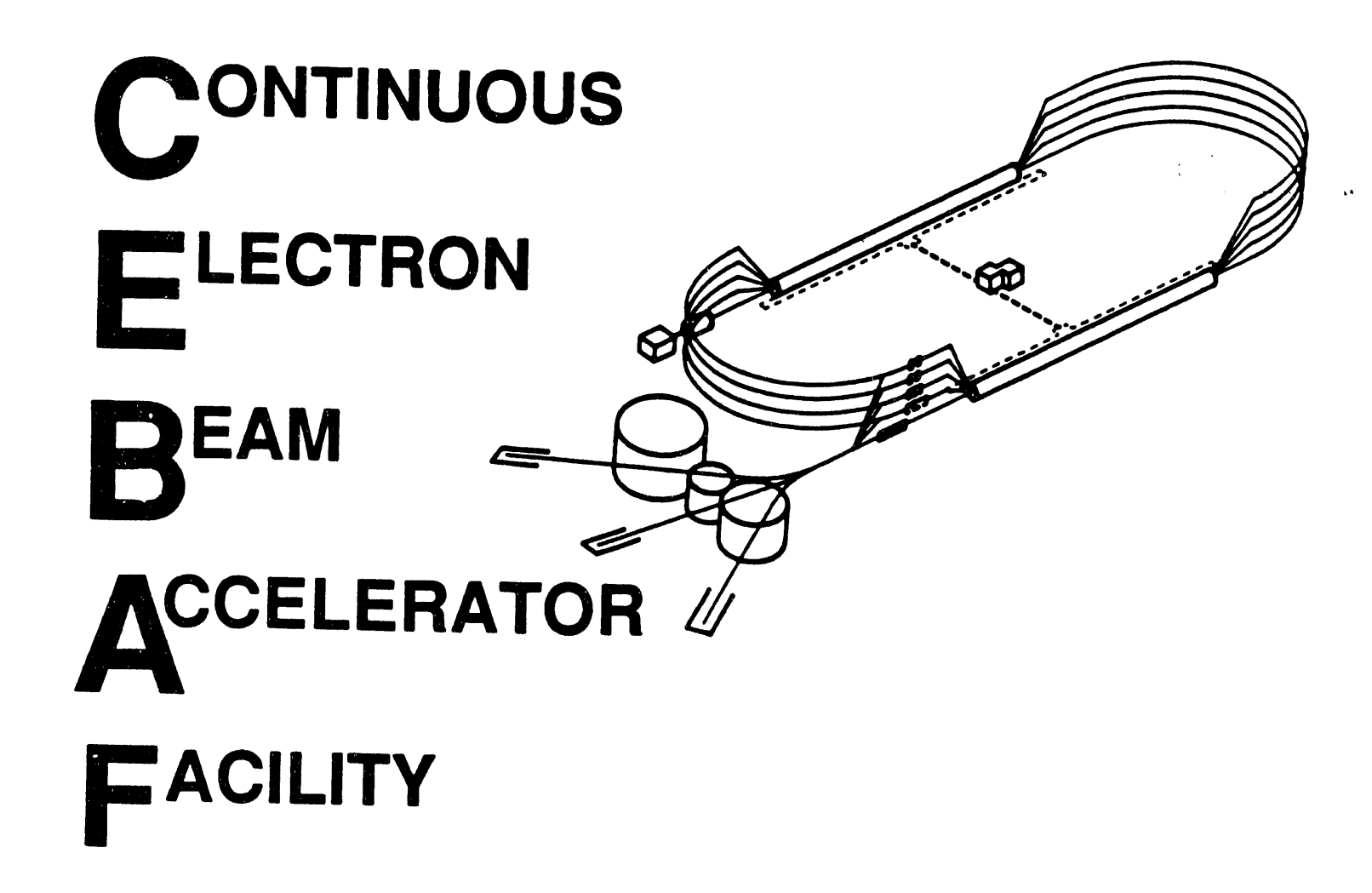


DOE/ER/40150--280 (CEBAP-R-93-001)

A BRIEF SUMMARY ON HMS OPTICS AND HALL C BEAMLINE INSTRUMENTATION

C. Yan. Physics Division. CEBAF

July 20, 1993



SURA Southeastern Universities Research Association

GEBAF

Newport News, Virginia

MASTER

942

Copies available from:

Library
CEBAF
12000 Jefferson Avenue
Newport News
Virginia 23606

The Southeastern Universities Research Association (SURA) operates the Continuous Electron Beam Accelerator Facility for the United States Department of Energy under contract DE-AC05-84ER40150.

DISCLAIMER

This report was prepared as an account of work sponsored by the United States government. Neither the United States nor the United States Department of Energy, nor any of their employees, makes any warranty, express or implied, or assumes any legal liability or responsibility for the accuracy, completeness, or usefulness of any information, apparatus, product, or process disclosed, or represents that its use would not infringe privately owned rights. Reference herein to any specific commercial product, process, or service by trade name, mark, manufacturer, or otherwise, does not necessarily constitute or imply its endorsement, recommendation, or favoring by the United States government or any agency thereof. The views and opinions of authors expressed herein do not necessarily state or reflect those of the United States government or any agency thereof.

A BRIEF SUMMARY ON HMS OPTICS AND HALL C BEAMLINE INSTRUMENTATION

C. Yan, Physics Division, CEBAF

1. Modification of HMS Optics

On June 19, 1992 we redefined HMS geometry based on two facts:

1. Having considered that the physical apertures of HMS elements are formed by the warm bore apertures of the cryomodule in the quads and the boundary of the vaccum chamber in the dipole magnet we set up a standard HMS geometry as shown in Figure 1. The effective lengths, physical apertures, and the equivalent lengths of the aperture collimators are listed in the Table 1.

Table 1. Physical apertures of HMS elements

| Element | Effective Length | Physical A | Referece Field | |
|---------|------------------|--------------------|----------------|---------|
| | (cm) | Diameter (cm) | Length (cm) | (Tesla) |
| Q1 | 189.0 | 40.515 | 237.2 | 1.508 |
| Q2 | 215.5 | 59.68 | 266.0 | 1.5293 |
| Q3 | 218.6 | 59.68 | 266.0 | 0.7721 |
| Dipole | 525.59 | 68.6×40.0 | 617.92 | 1.6567 |

2. The final drift distance from the EFB of the dipole exit to the midpoint of the two wire chambers was reduced from 725 cm to 625 cm duo to the limited space in the shielding house for the 100 cm elongation of detector package (mainly, duo to the elongation of the Cherenkov counter).

The TRANSPORT input data deck of HMS with physical aperture is listed in Table 2.

Table 2. TRANSPORT Input Data Deck for HMS-1

```
'HMS-1 WITH MODIFIED PHYSICAL DIMENSION.
                                                                          0.0
         82.5
                                           'BEAM':
                                          '2-ND'
                                                               0
5.01
                  15.07763
                                 25.
         1.2275
                                                                                   0.000001
                     -15.85514
                                    35.
                                                                                   0.000001
                                                                           -0.12
5.01
                    7.70992
                                  35.
         2.186
                                                      SENTINEL
```

Table 3. HMS Field Setting and First-Order Performances in Normal Modes

| | HMS-1 | HMS-2 | HMS-3 |
|-----------------------------|-------------------------|----------------------|----------------------------|
| $B(Q_1)$ in kG | 15.04159 | 14.65548 | 14.82348 |
| $B(Q_2)$ in kG | -15.64286 | -14.21163 | -14.82344 |
| $B(Q_3)$ in kG | 7.82593 | 7.52250 | 7.65426 |
| B(dipole) in kG | 16.6 | 16.6 | 16.6 |
| R_{11} | -3.09071 | -3.09071 | -3.09071 |
| R_{16} | 3.70886 | 3.70886 | 3.70886 |
| R_{22} | -0.32355 | -0.32355 | -0.32355 |
| R_{26} | 4.12725 | 4.12725 | 4.12725 |
| R_{33} | -2.63851 | 0.0 | -1.10726 |
| R_{44} | -0.37900 | 0.27525 | 0.0 |
| R_{52} | -0.12 | -0.12 | -0.12 |
| L in m (for p_o) | 23.06 | 23.06 | 23.06 |
| θ acceptance in mr | $\pm~82.5$ | $\pm~82.5$ | \pm 82.5 |
| φ acceptance in mr | ± 22.0 | $\pm \ 22.0$ | $\pm \ 22.0$ |
| Ω in msr | 5.70 | 5.70 | 5.70 |
| Target length in cm | ± 5 | ± 5 | ± 5 |
| Momentum range in% | ± 10 | ± 10 | . ± 10 |
| Constraints | $x/\theta = y/\phi = 0$ | $x/\theta = y/y = 0$ | $x/\theta = \phi/\phi = 0$ |
| Imaging mode | Pt-Pt | Para-Pt | Pt-Para |

where the solid angle is estimated by an open ellipsoidal cone with open angles $2\theta_{max}$ and $2\phi_{max}$ from the vertex and then $\Omega = \pi\theta_{max} \times \phi_{max}$.

Enge's fringing field approximation is an intermediate step to transfer field setting from TRANSPORT to RAYTRACE. The input data deck is shown in Table 4.

Table 4. TRANSPORT Input Data Deck with Enge's Fringing Field Approximation

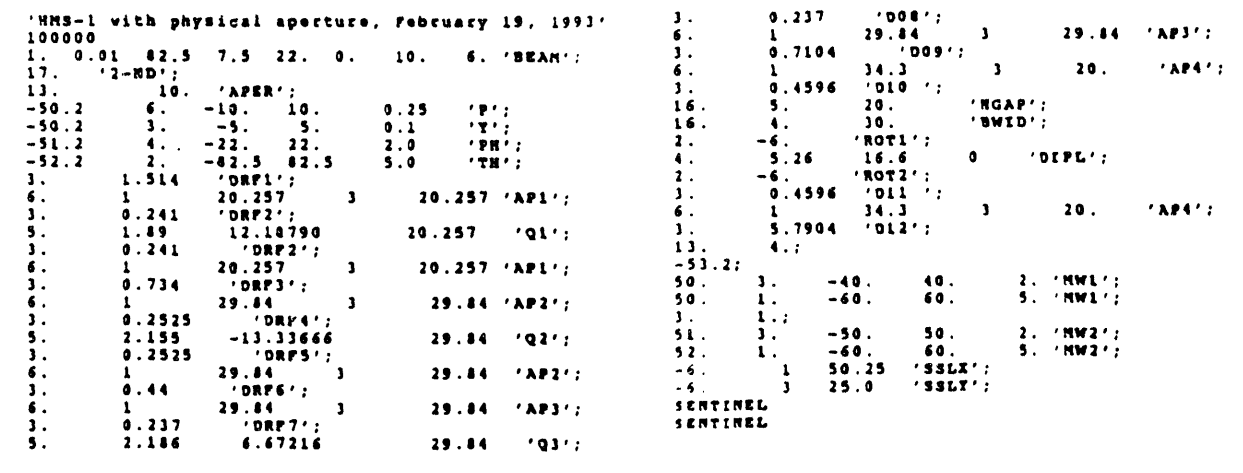
| | l with Enge | 's FF Approxi | mation, | June 24 | | | | | | |
|-------------------|-----------------|---------------|---------|--------------------|------------|-----------------|----------|------------------|----------|--------------------|
| 0. 1. 0 17. | .01 82.5 | 5. 22. 0. | 5. 6. | 'BEAM'; '2-ND'; | 5.0C | 1.836 | | 7.7099 7.7099 | | 'Q003'; 'Q003'; |
| 3. | 1.755 | | | 'DRF1'; | 3. 3. | -0.175 1.407 | • | | | 'DRF4'; |
| 3. 5.0a | -0.125; 0.25 | 17.5 | 50. | 'Q001'; | 16. | 5. | | 21. | | 'BGAP'; |
| 5.0A | 1.64 | 17.5 | 25. | 'Q001'; | 16. 16. | 12. 13. | | 0.0 | | '1/R1'; '1/R2'; |
| 5.0A 3. | 0.25 -0.125; | 17.5 | 50. | 'Q001'; | 2. | -6.0 | | | | 'ALPH'; |
| 3. | 1.2275 | | | 'DRF2'; | 4. | 5.26 -6.0 | | 16.6 | 0.0 | 'DIPL'; 'BETA'; |
| 3. 5.0B | -0.175; 0.35 | -15.85514 | 70. | 'Q002'; | 3. | 6.25 | , | • | | 'DRF5'; |
| 5.0B | 1.805 | -15.85514 | 35. | 'Q002'; | 10. 10. | -1. -3. | 2. 4. | 0. 0. | 0.000001 | 'FIT1'; 'FIT2'; |
| 5.0B 3. | 0.35 -0.175: | -15.85514 | 70. | 'Q002'; | 10. 13. | -5 . | 2. | -0.12 | 0.000001 | 'FIT3'; |
| 3. | 0.9295 | | | 'DRF3'; | 3. | 4.; 5. 'DRF | 6′; | | | |
| 3. 5.0c | -0.175; 0.35 | 7.70992 | 70. | 'Q003'; | SENT | | | | | |

Table 5. HMS Field Setting and First-Order Performances in Normal Modes with Enge's FF approximation

| | HMS-1 | HMS-2 | HMS-3 |
|---------------------|-------------------------|----------------------|----------------------------|
| $B(Q_1)$ in kG | 15.17658 | 14.78658 | 14.95492 |
| $B(Q_2)$ in kG | -15.82056 | -14.38752 | -14.99533 |
| $B(Q_3)$ in kG | 7.90786 | 7.60102 | 7.73345 |
| B(dipole) in kG | 16.6 | 16.6 | 16.6 |
| R_{ii} | -3.09071 | -3.09071 | -3.09071 |
| R_{16} | 3.70886 | 3.70886 | 3.70886 |
| R_{22} | -0.32355 | -0.32355 | -0.32355 |
| R_{26} | 4.12725 | 4.12725 | 4.12725 |
| R_{33} | -2.63766 | 0.0 | -1.10157 |
| R_{44} | -0.37912 | 0.27307 | 0.0 |
| R_{52} | -0.12 | -0.12 | -0.12 |
| L in m | 23.06 | 23.06 | 23.06 |
| Ω in msr | 5.70 | 5.70 | 5.70 |
| Target length in cm | ± 5 | ± 5 | ± 5 |
| Momentum range in% | ± 10 | ± 10 | ± 10 |
| Constraints | $x/\theta = y/\phi = 0$ | $x/\theta = y/y = 0$ | $x/\theta = \phi/\phi = 0$ |
| Imaging mode | Pt-Pt | Para-Pt | Pt-Para |

In order to obtain HMS transmissions, TURTLE code is used to generate a fast histogram display which is based on second-order optics. In TURTLE type code 13.0 causes the program to observe magnet apertures. If 13.0 code is present, the program will terminate all those rays which pass outside the specified apertures of quadrupoles or bending magnets. The quadrupole half aperture is normally taken to be circular and equal to the fourth entry on the type cade card. To meet the physical aperture, both of the field at the pole tip and the radius of quadrupole must be modified as displayed in Table 6.

Table 6. HMS TURTLE Input Data Deck



In Figure 2 and Figure 3, a series of beam envelopes from TURTLE output is given. In these figures, the features of HMS collective collimator (physical aperture) is clearly displayed. The design of vaccum chamber of dipole magnet as well as the vaccum pipe which connects dipole outlet with the detector section is based on those calculations.

In RAYTRACE code the physical aperture is simulated by placing collimators before, after, and in the middle of element (by using a negative drift distance) as shown in Table 7. Though the simulation of physical aperture by collimators is not as good as what are defined in TURTLE code, most of passing behaviours of a bundle of rays can be described precisely.

Table 7. HMS RAYTRACE Input Data Deck with Physical Apertures

```
HMS-1 (point-to-point) October 28 10.500,0,2
                                                                            0.1451, 6.3414, -1.9308, 0.2696
0.1451, 6.3414, -1.9308, 0.2696
1., 1.,1., 1.
DRIF
6000.,300.,1.
DRIF
151.4
                                                                             -109.3
                                                                            COLL
1.,0.,0.,20.257,20.257
                                                                            1.,0.,0.,29.84,29.84
DRIF
                                                                            109.3
                                                                            COLL
1.,0.,0.,20.257,20.257
                                                                            1.,0.,0.,29.84,29.84
DRIF
POLES
POLES
8.,8.,8.
0.,0.,189.,25.
1.5269
75.,-60.,-60.,75.
                                                                           1.,0.,0.,29.84,29.84
DRIF
71.04
0.0688, 6.2624, -1.0500, 0.788
0.0688, 6.2624, -1.0500, 0.788
                                                                           COLL
1.,0.,0.,34.3,20.
DRIF
1.,0.,0.,20.257,20.257
DRIF
                                                                            45.96
                                                                           COLL
1.,0.,0.,34.3,20.
DIPOLE
1.,0.,0.,20.257,20.257
                                                                           DIPOLE
12.5,12.5,12.5,12.5,1.
0.0.,42.0,1205.5,1.66035
25.,-6.,-6.
1.,0.,0.,29.84,29.84
                                                                           0.
120.,-100.,-100.,120.0
0.09030, 3.00572, -0.28534, -0.045, 0.02918
0.09030, 3.00572, -0.28534, -0.045, 0.02918
DRIP
COLL
POLES
10.,10.,10.
0.,0.,215.5,35.
-1.58757
                                                                           COLL
1.,0.,0.,34.3,20.
DRIF
-1.58757
140.,-65.,-85.,140.
0.1014. 6.0266, -1.2084, -0.0928
0.1014. 6.0266, -1.2084, -0.0928
1.,1.,1.,1.
DRIF
-107.75
                                                                           COLL
                                                                           1.,0.,0.,34.3,20.
DRIF
                                                                            579 04
COLL
1.,0.,0.,29.84,29.84
DRIF
                                                                           SENTINEL
107.75
COLL
1.,0.,0.,29.84,29.84
DRIF
25.25
1.,0.,0.,29.84,29.84
DRIF
1.,0.,0.,29.84,29.84
DRIF
1.,0.,0.,29.84,29.84
POLE
10.,10.,10.
0.,0.,218.6,35.0
0.79128
140.,-85.,-85.,140.0
```



2. Special Tuning of HMS

2-1. Limit parameters from TOSCA

A set of limit parameters of HMS quadrupoles from TOSCA calculation is listed in Table 8.

Table 8. Limit parameters from TOSCA design

QUADRUPOLE 1

| Maximum cryostable current (Ampere/turn) | 1089.6 |
|--|-----------------------------|
| Effective length at 1089.6 (meter) | 1.877 (100% packing factor) |
| | 1.870 (96% packing factor) |
| Integral quadrupole field (Tesla-m) | 3.4232(100% packing factor) |
| at pole radius | 3.4300(96% packing factor) |
| Central gradient at R=22 cm (Tesla/m) | 7.294 (100% packing factor) |
| | 7.3357(96% packing factor) |
| Maximum field at pole radius (Tesla) | 1.8235(100% packing factor) |
| | 1.8339(96% packing factor) |

QUADRUPOLE 2,3

| Maximum cryostable current (Ampere/turn) | 1089.6 |
|--|-----------------------------|
| Effective length at 1089.6 (meter) | 2.102 (100% packing factor) |
| | 2.083 (96% packing factor) |
| Integral quadrupole field (Tesla-m) | 4.5158(100% packing factor) |
| at pole radius | 4.5366(96% packing factor) |
| Central gradient at R=22 cm (Tesla/m) | 6.1448(100% packing factor) |
| | 6.2310(96% packing factor) |
| Maximum field at pole radius (Tesla) | 2.1507(100% packing factor) |
| | 2.1809(96% packing factor) |

2-2. 7.5 GeV/c HMS

Second order TRANSPORT: Q_1 is fixed at 1.75 Tesla, adjust Q_2 and Q_3 to satisfy the desired imaging mode.

Table 9. Field setting of 7.5 GeV/c HMS

| | | | | | | | 1 | | | |
|-------|--|--------------|------|-------|------|------|---|------|------------|--|
| Kriti | | 11 11 11 | ar I | lli i | | | | h.,. | ا السلام ا | |

| | HMS-1 | HMS-2 | HMS-3 |
|-------------------------|------------|------------|------------|
| $B(Q_1)$ in kG | 17.5 | 17.5 | 17.5 |
| $B(Q_2)$ in kG | -19.59979 | -17.70097 | -18.62028 |
| $B(Q_3)$ in kG | 10.36460 | 9.76748 | 10.06587 |
| B(dipole) in kG | 20.75 | 20.75 | 20.75 |
| D/M | -1.4919 | -1.3699 | -1.4286 |
| θ acceptance in mr | ± 72.5 | ± 72.5 | ± 72.5 |
| ϕ acceptance in mr | ± 25.0 | ± 25.0 | ± 25.0 |
| Ω in msr | 5.69 | 5.69 | 5.69 |
| Target length in cm | ± 5 | ± 5 | ± 5 |
| Momentum range in% | ± 5 | ± 5 | ± 5 |

The current 7.5 GeV/c HMS is different to the original 7.4 GeV/c mode reported in HMS manual [1] because no displacement of quadrupoles is required.

2-3. 10 msr HMS

Second order TRANSPORT: Q_1 is fixed at 1.75 Teslacional electriplet is moved towards the target for 40 cm, adjust Q_2 and Q_3 to satisfy the desired imaging mode.

Table 10. Tuning parameters of 10 msr HMS

| | HMS-1 | HMS-2 | HMS-3 |
|---------------------------|------------|------------|--------------|
| $B(Q_1)$ in kG | 17.5 | 17.5 | 17.5 |
| $B(Q_2)$ in kG | -16.07957 | -14.76459 | -15.25068 |
| $B(Q_3)$ in kG | 7.87284 | 7.39865 | 7.58060 |
| B(dipole) in kG | 16.6 | 16.6 | 16.6 |
| D/M | -1.0103 | -0.9321 | -0.9608 |
| heta acceptance in mr | ± 95.0 | ± 99.0 | ± 99.0 |
| ϕ acceptance in mr | ± 35.0 | ± 30.0 | $\pm \ 35.0$ |
| Ω in msr | 10.44 | 9.33 | 10.88 |
| Target length in cm | ± 1 | ± 1 | ± 1 |
| Momentum range in% | ± 5 | ± 5 | ± 5 |

There is no interference of fringing field at the target chamber region. The contribution of fringing field of Q_1 on the target position is still zero.

2-4. QQD Variation

A QQD structure of HMS is still working while the first quadrupole is shut down or moved away. There are also three possible tunes in transverse plane: point-to-point, parallel-to-point, and point-to-parallel.

Table 11. Tuning parameters of QQD variation

| | QQD-1 | QQD-2 | QQD-3 |
|---------------------|------------|------------|------------|
| $B(Q_1)$ in kG | 0. | 0. | 0. |
| $B(Q_2)$ in kG | 13.63836 | 13.27144 | 12.72918 |
| $B(Q_3)$ in kG | -10.69976 | -9.63605 | -8.20826 |
| B(dipole) in kG | 16.6 | 16.6 | 16.6 |
| D/M | -0.7499 | -0.7931 | -0.8580 |
| θ acceptance in mr | ± 67.0 | ± 67.0 | ± 67.0 |
| φ acceptance in mr | ± 15.0 | ± 15.0 | ± 15.0 |
| Ω in msr | 3.16 | 3.16 | 3.16 |
| Target length in cm | ± 1 | ± 1 | ± 1 |
| Momentum range in% | _ ± 5 | ± 5 | ± 5 |

For the QQD variation of HMS, the third order correction has to be used to compensate the large chromatic aberration caused by doublet system. The Table 12 shows image distribution along focal plane in RAYTRACE frame and that is also an indication of systimatic momentum resolution (in reconstructed).

Table 12. Image distribution of QQD

| $\delta = \Delta p/p \text{ in } \%$ | -5.0 | -2.5 | 0. | 2.5 | 5.0 | $\Omega(\mathrm{msr})$ | Correction |
|--------------------------------------|-------|--------|--------|--------|--------|------------------------|------------|
| ΔX_{max} in cm | 9.111 | 10.494 | 12.412 | 15.219 | 19.680 | 6.4 | no |
| ΔX_{max} in cm | 3.689 | 4.233 | 4.991 | 6.103 | 7.873 | 2.92 | no |
| ΔX_{max} in cm | 1.210 | 0.947 | 0.609 | 0.316 | 1.034 | 6.4 | yes |
| ΔX_{max} in cm | 0.390 | 0.283 | 0.147 | 0.125 | 0.446 | 2.92 | yes |

The ratio of the octapole component to the quadrupole: 1.01% for Q_2 and 2.05% for Q_3 . The beam envelopes of QQD-1, QQD-2, and QQD-3 are displayed in Figure 4, Figure 5, and Figure 6. The image behaviour of QQD is shown in Figure 7.

2-5. Inversed triplet tuning

R. Madey in his G_E^n proposal asks for a large acceptance in the transverse plane and this could be realized by alternately setting the polarities of Q1, Q2, and Q3. The setting parameters in this mode are listed in Table 13. The envelope of HMS with alternate triplet polarities is shown in Fig. e 8. The momentum acceptance, angular acceptances are shown in Figure 9, 10, 11, respectively.

Table 13. TURTLE parameters of HMS with alternate triplet polarities



```
'Inversed triplet,
100000
            22.5
                    5.0
                          62.
                                0.
                                                'BEAM';
             10
                   -5.
-5.
            6.
                                     0.25
                                              'P';
                                     0.1
                                              'Y'
                                              'PH':
                                     2.0
                   -22.5
                                              TH'
          1.514
                    20.257
                                 3
                                         20.257 'AP1';
          0.241
          1.89
                                         20.257
                                                   'Q1';
          0.241
          0.734
3.
          0.2525
          2.155
                      12.78857
                        DRF5
                                         29.84
3.
          0.237
                       DRF7
          2.186
                                         29.84
          0.237
                     'D08';
          0.7104
                        ' D09
                    34.3
                                         20.
                                                  'AP4';
                    ' D10
16
                    20.
                               'HGAP';
16.
                    30
                                BWID';
                   ROTI
          5.26
                    16.6
                               0
                                     'DIPL':
          0.4596
                    'D11
                    34.3
                                         20.
          5.7904
                    'D12';
13
          4.;
-53.2:
        3.
                -40
                          40.
52.
                -60.
                          60.
                                       'MWI'
                -50.
                          50.
                                        MW2';
52.
                -60.
                          60.
                50.25
25.0
                         SSLX';
                         'SSLY':
SENTINEL
SENTINEL
```

3. Hall C beam transport line

The Hall C beam transport lines consists of the separation section, the first match section which match the separator to the arc, the arc section and the second match section matching arc to the target with total length of 146.2 m from the point of tangency to the Hall C target position, including eight 3 meter bending dipole magnets, two 1 meter separation magnets, twenty one 30 cm quadrupole magnets, eight sextupole magnets and several beam correctors distributed along the arc section.

CEBAF beam is transported by waist-to-waist imaging to the point of tangency point, then it is separated by separation section into Hall A, Hall B, and Hall C respectively. Through the first match section the separated Hall C beam enters into the arc section which achromatically bends the beam by 34.3° with a

radius of 40 meters and the second match section sends recombined beam to Hall C target position through a distance of 179.47 feet.

The arc section consists of eight 3 meter length dipole magnets (BA), 11 quadrupoles (QA) with 2.54 cm aperture and 8 sextupoles which provide a complete second order achromatic transport - both of the dispersion and its derivative must be zero. Therefore, the first half of achromat focuses second principal plane of the fourth bending magnet onto the first principal plane of the fifth bending magnet. The effect of the intermediate quadrupole is solely to achieve complete recombination of different momenta.

If the half width of the source is x_0 , the the full width of the image is $2x_0M_x$, two different momenta can be resolved if their spatial separation is at least as great as the width of the image of the source. Therefore, momentum resolution is defined as:

$$R_p = \frac{\Delta P}{P} = \frac{2M_x x_o}{D}$$

 M_x - magnification in x-direction, D - dispersion in transverse direction. Different momenta can be separated at the intermediate focal plane of arc achromat that is so-called a bean line spectro meter combination in what is known as the energy-loss mode. At the intermediate focal plane of Hall C arc achromat the dispersion is 2.078 cm/% and magnification is about unit. If a focal plane detector can be placed at the midpoint it will be a high resolution achromatic spectrometer that can be used to analyse a relative beam momentum deviation.

The second match section consists of 5 quadruples Q_{17} , Q_{18} , Q_{19} , Q_{20} and Q_{21} . This 5 quads cluster execute three functions: 1. In normal operation, achromatically focus the beam onto the target with double point-to-point imaging; 2. with seriesly powered $Q_{17} - Q_{18}$ and $Q_{20} - Q_{21}$, the beam can be defocused with an arbitrary beam spot size, for example, 2.5×2.5 cm² for polarized target, $2.5 \times$ $0.01~\mathrm{cm^2}$ for high resolution operation of either SOS or HMS, and $0.1\times0.1~\mathrm{cm^2}$ for HMS cryogenic target; The results of TURTLE simulations show the two dimentional beam density distribution under the defocusing function. Notice that the variable defocusing properties are approximately achromatic transport in the first order ($\sim 1\%$). This function is used as an emergency protection for Hall C raster system which will be replaced by the defocusing quads cluster as soon as any failure of the raster system occurs; 3. when there is either a dummy target cell or no target in site, the quads cluster sends a defocusing beam to the beam dump through the tunnel with 4×4 cm² spot size. The beam density distributions on the target under different defocusing operations are obtained from TURTLE runs and are displayed in Figure 13, 14, 15, and 16. The defocusing features of 5 quads cluster are listed in Tabel 14. The second card in a TRANSPORT deck contains an integer which serves as an indicator. When using TURTLE this card constrains an integer indicating how many rays one wishes to run through the system. With a minor modification (2-nd entry card and switch on code 50. cards) the TRANSPORT input deck can be used for TURTLE calculations. The TURTLE input data deck for Hall C beam line is listed in Table 15. A 4.665 m

reduction in the total length has been applied to the original Hall C beam line deck. This difference comes from the offset of the target position to the geometric center of Hall C.

As a part of Hall C safe operations, the defocusing features of the quadrupole cluster can sufficiently protect target materials from overheating effect. There are, of course, several disadvantages such as: non-uniform beam density distribution within the beam spot; degeneration of spectrometer resolution due to the blur of beam image on the target; blow-up of reconstruction accuracy.

In order to simplify operation tunings for the quadrupole cluster a special connection between Q_{18} , Q_{19} , Q_{21} , and Q_{22} are required. The Q_{18} , Q_{19} pair are inversely connected with Q_{21} , Q_{22} pair and therefore, there are only two adjustable parameters in this section as listed in Table 14.

Table 14. Defocusing Features of the Last 5 Quads

| $\Delta x_{target} (cm)$ | 0.0098 | 0.1 | 1.25 | 1.25 |
|--------------------------|------------|------------|------------|----------|
| Δy_{target} (cm) | 0.0361 | 0.1 | 1.25 | 0.1 |
| Δx_{dump} (cm) | 0.0689 | 0.4332 | 4.3825 | \$.9630 |
| Δy_{dump} (cm) | 0.1344 | 0.3298 | 4.0171 | 0.4013 |
| $B_{Q_{18,19}}$ in kG | -0.74567 | -1.19053 | -3.58606 | -2.76379 |
| $B_{Q_{20}}$ in kG | -0.30622 | 0.19323 | -1.25574 | 1.66338 |
| $B_{Q_{21,22}}$ in kG | 0.74567 | 1.19053 | 3.58606 | -2.76379 |
| R_{16} | -0.00011 | 0.00130 | -0.01629 | 0.01631 |
| R_{26} | 0.00019 | 0.00084 | -0.00794 | 0.00689 |
| Applications | Achromatic | HMS target | UVa target | SOS-HNSS |

Table 15. TURTLE input deck of Hall C beam line

```
'Modified Hall C Beam
                                       June 16, 1993'
    0.010
             0.010
                      0.010
                               0.010
                                        0.000
                                                 0.01
                                                         6.000
                                                                 'BEAM';
     0.4500
              'D001'
                     ;
     0.0000
               -5.5889
     1.0000
                            0.0000
                                     'B001' ;
    -1.6000
    12.0000
               'D002'
                 1.6356
      0.3000
                             1.2500
                                      'Q001';
     2.0000
               ' D003'
               -2.5731
     0.3000
                            1.2500
3
     2.0000
               D004'
      0.3000
                  1.6356
      .0000
               'D005';
    -1.6000
     1.0000
               -5.5889
                            0.0000
                                     'B002' ;
     0.0000
              ' D006'
     1.0000
      9.3000
                 2.50850
                              1,2500
               D007'
     5.0000
      0.3000
                 -2.3090
                            1.2500
     5.0000
               D008'
      0.3000
                 2.5518
     5.0000
              ' D009'
      0.300
               -3.2939
                         1.2500
```

```
-2.29710
          'D010';
                                                   5.
                                                         0.3000
                                                                                1.2500
                                                                                        'Q013';
     5.0
     0.4
          '0011';
                                                        0.4000
                                                                  D034'
                                                   3
3.
                                                   18
                                                         0.3000
                                                                   -0.02760
                                                                                1.2500
                                                                                        'S006';
13.
     1.;
                                                        0.4000
                                                                 'D035'
13.
     4. :
             2.
                  0.
                       0.00001 'FT01';
                                                       -2.1437 ;
-10.
                  0.
                       0.00001 'FT02';
                                                        3.0000
                                                                  -4.9922
                                                                              0.0000
                                                                                      'B008';
      -2.
            1.
-10.
                       0.00001 'FT03';
                  0.
                                                       -2.1437
      - 3 .
-10.
             4.
                                                                 'D036';
                       0.00001 'FT04';
                  0.
                                                        0.4000
-10.
      -4.
             3.
                                                                 ' D037'
             'D012':
     0.4
                                                        0.4000
3.
     0.30
              2.31120
                             1.25
                                     'Q008';
                                                        0.3000
                                                                   2.31120
                                                                               1.2500
                                                                                       'Q014' ;
5.
     0.4000
             'D013'
                                                                 ' B038'
                                                        0.4000
3
       0.3000
                                                                    0.01580
                  0.01580
                              1.2500
                                     '5001';
                                                         0.3000
                                                                                1.2500
                                                                                         'S007' ;
                                                   18
18.
             'D014';
                                                                 'D039';
                                                        0.4000
     0.4000
3
                                                       -2.1437 ;
    -2.1437 ;
                           0.0000
                                   '8003';
                                                        3.0000
                                                                  -4.9922
                                                                              0.0000 '8009';
               -4.9922
     3.0000
                                                       -2.1437 ;
    -2.1437 ;
                                                                 'D040';
             'D015';
                                                        0.4000
     0.4000
                                                                 'D041'
              '0016'
                                                        0.4000
     0.4000
                -2.2971
                                                                   -2.29710
                                                                                1.2500
5 .
      0.3000
                           1.2500
                                    'Q009';
                                                   5.
                                                         0.3000
                                                                                         '0015' :
                                                        0.4000
                                                                 'D042'
     0.4000
             '0017'
                                                   3
                -0.02760
                                                                 -0.02760
                                       'S002' :
                                                         0.3000
                                                                                         'S008' ;
18.
       0.3000
                              1.2500
                                                   18
                                                                                1.2500
             'D018';
                                                        0.4000
                                                                 'D043';
     0.4000
                                                   3
    -2.1437 ;
                                                       -2.1437
     3.0000
               -4.9922
                           0.0000 '8004';
                                                        3.0000
                                                                  -4.9922
                                                                              0.0000 '8010' :
    -2.1437 ;
                                                       -2.1437
                                                                 'D044';
     0.4000
             'D019';
                                                        0.4000
                                                                 'D045'
     0.4000
              ' D0 20 '
                                                        0.4000
      0.3000
                 2.31120
                             1.2500
                                      '0010' :
                                                        0.15
                                                                 2.31120
                                                                            1.2500 'Q016';
             ' D0 21 '
                                                   13.
     9.4000
                                                           4.;
       0.3000
                  0.01580
                              1.2500
                                       'S003' ;
                                                   13.
              'D022';
                                                                   2.
                                                                          0.
                                                                                0.00001
                                                                                           'FT09':
     0.4000
                                                   -10.
                                                                          0.
                                                            -3.
                                                                                0.00001
                                                                                           'FTLO';
    -2.1437 ;
                                                   -10.
                                                                   4.
                                                            -1.
     3.0000
               -4.9922
                           0.0000 '8005';
                                                   -10.
                                                                          0.
                                                                                0.00001
                                                                                           'FT11';
    -2.1437 ;
                                                           -2.
                                                                                           'FT12';
                                                   -10.
              'D023'
                                                   5.
                                                        0.15
                                                                 2.12530
                                                                           1.2500
                                                                                     'Q016';
     0.4000
     0.4000
              ' DQ 24 '
                                                        2.5000
                                                                'D046';
      0.3000
                 -2.2971
                            1.2500
                                     'Q011';
                                                         0.3
                                                                -1.17940
                                                                             1.2500 'Q017';
              'D025';
                                                                   100471;
     0.4000
                                                        15.1
18.
       0.3000
                -0.02760
                             1.2500
                                      'S004';
                                                   5.0A
                                                            0.3
                                                                                  'Q018';
     0.4000
              'D026';
                                                                   'D049';
                                                            0.5
                                                                   -3. 1.25
    -2.1437 ;
                                                   5.0A
                                                            0.3
                                                                                  '0019':
                                                                    100491
                           0.0000 '8006';
     3.0000
               -4.9922
4
                                                   5.01
                                                                0.3
                                                                     -0.63691 1.2500 'Q020';
     -2.1437 :
     0.800 '0027' ;
                                                                    'D050'
13. 4.;
                                                   5.0-A
                                                            0.3
                                                                            1.25
                                                                                      'Q021';
                                                         0.5
                                                                 'D051';
13. 1.;
                                                                                     'Q022';
       0.1500
                2.31120
                            1.2500
                                     'Q012';
                                                   5.0-A
                                                               0.3
                                                                 'D053';
                                                          22.
13.
       4. ;
                                                   3.
                                                   -10.
                                                                2. 0.
                                                                           0.00001 'FT20';
                                                          -1.
13.
      1. ;
                                                                4.
        -2.
              6.
                   O.
                            0.00001
                                       'FT05';
                                                   -10.
                                                         -3.
                                                                           0.00001 'FT21';
-10.
                            0.00001
                                       'FT06';
                                                         -1.
                                                                           0.00001
                                                                                   'FT22';
              2.
                                                   -10.
-10.
        -1.
                   0.
                                       'FT07';
                                                        1.
                                                             1. 1.25
3. 1.25
                                                                                    'FT23';
                            0.00001
                                                                          0.00001
                                                   10.
        -3.
-10.
              4 .
                    0.
                                                                                    'FT24';
                            0.00001
                                       'FT08';
                                                                          0.00001
                   0.45
-10.
        -5.
              2.
                                                   10.
                                                         3.
                                                                                           'Y';
                                                                  -2.5
                                                                                     0.25
                                     'Q012'
                                                            3.
                                                                            2.5
5.
      0.1500
                2.31120
                            1.2500
                                                   -52.
                                                   -51.
                                                                                          'X';
13.
      4.;
                                                            1.
      1.;
                                                        1.;
13.
                                                   13.
              'D029';
                                                         4 . ;
3
      0.4
                                                   13.
                 0.01580
                                                          27.07
       0.3000
                             1.2500
                                      'S005';
                                                                 'D054';
                                                   3.
18
              'D031';
3
      0.4000
                                                   13.
                                                        1.;
                                                         4.;
     -2.1437
                                                   13.
               -4.9922
                           0.0000 '8007';
                                                                 'DUMP':
                                                   3.
      3.0000
                                                         1.;
                                                   13.
     -2.1437 ;
2
                                                   13.
              'D032';
      0.4000
                                                   SENTINEL
               'D033';
      0.4000
                                                   SENTINEL
```

4. Beam Energy Measurement by Arc Spectrometer

Beam energy measurement by the arc spectrometer was proposed and de-

veloped in refs. [2], [3], [4], and [5]. Hall C achromatic beam transport line will be used as a spectrometer which has a dispersion of 12 cm/% with all the quadrupoles, sextupoles, and beam correctors switched off. The beam envelope of arc spectrometer is shown in Figure 17. The transverse position and the angle of the beam at the entrance of the arc are precisely measured by a pair of wire scanners spaced by 2.5 m, and the transverse position of the outgoing beam is measured by another pair of wire scanners at the exit of the arc. From these positions and the calibrated bending field in the dipoles, an absolute beam energy is measured. After the absolute beam energy is measured, the arc will be turned into the normal achromatic mode by energizing all the elements. The beam position probe located at the mid-point of the arc will be used to monitor the beam energy in this operational mode. A complete error analysis shows that an absolute beam energy measurement with 10⁻³ accuracy can be achieved. Relative energy measurements at the 10⁻⁴ level are also obtainable.

The position and the direction of the beam entering the Hall C arc line are determined at the entrance by a pair of high-resolution harps (wire scanners). The position (and direction) of the beam at the exit of the 34.3° bend (41.6 m downstream from the point of tangency) is determined by another pair of calibrated harp(s). For this procedure only the dipoles are energized. During this absolute measurement all other arc magnetic elements such as quads, sextupoles, beam correctors are off. The current in the absolutely calibrated bending magnets is varied to set the position to be along the central ray of the magnets in the arc. With this information, the beam momentum is determined. Thus, this method requires accurate position (and implicitly direction) measurements at the harps and an accurate determination of the magnetic field integral $\int Bdl$ as a function of current I in the arc dipoles.

The quadrupoles and sextupoles are then energized to the values required by the measured energy in the normal achromatic transportation mode. The orbit correctors are activated to center the beam on a beam position measuring device situated at the midpoint of the achromat. Under the assumption that the beam momentum is unchanged during this transition period, we can transfer the absolute momentum calibration to the achromatic mode, which is very sensitive to relative shifts in the beam momentum. Variations in beam energy can then be measured as variations in beam position at the midpoint. This achromatic mode will also be capable of obtaining relative energy measurements with substantially greater accuracy than the absolute mode. Subsequent error analyses obtained from DIMAD and RAYTRACE are shown in the table.

Table 16. Error Sources Analyses

| Classified error source | Figures | Contribution |
|--|----------------------|-----------------------|
| Harp fiducialization error | $50~\mu m$ | 3.05×10^{-5} |
| Harp to harp survey error | $100~\mu m$ | 2.29×10^{-5} |
| Harp pair to harp pair survey error | $200~\mu m$ | 2.25×10^{-5} |
| Beam steering accuracy at the entrance | $100~\mu m$ | 3.5×10^{-4} |
| Beam steering accuracy at the exit | $100~\mu m$ | negligible |
| $\Delta \int Bdl/\int Bdl$ measurement error | 2.5×10^{-4} | 2.5×10^{-4} |
| Magnet positioning accuracy | 1 mm | 10-4 |
| Magnet orientation accuracy | 1 mr | 10-4 |
| Magnetic mispowerings (random) | 10-3 | 1.2×10 ⁻⁴ |
| Angle kick in the arc | 0.05 mr | 1.3×10^{-4} |
| Intermediate monument location accuracy | 20 μrad | 1.6×10^{-4} |
| Sink of support System | 2 mm in y | negligible |
| Thermal expension of support system | 2 mm in y | negligible |
| Beam initial emittance | 0.01 cm, 0.01 mr | 3.2×10^{-5} |
| Beam initial energy spread | 10-4 | 10-4 |

The analyses indicate that an absolute beam energy measurement at the 1.0 to 1.5×10^{-3} level is obtainable with high confidence. The proposed method will also be capable of obtaining relative energy measurements with substantially greater accuracy. In that mode the field normalization error is inapplicable and missteering effects are reduced (by the strong focusing and 180° entrance to arc center phase advance). The dominant error should be harp misalignment and measurement uncertainties. The sum of those errors should be less than $\delta x \sim 0.2$ mm. The resulting error in $\delta E/E$ (relative) will be on the level of $\delta x/D \sim 10^{-4}$. There is no need to change the hardware or the optical tuning of the achromat in the original beam line design. As the major precision beam position probe, the upgraded CEBAF harp or "Superharp", is developed and tested, a special alignment technique for the superharps must be carefully considered and implemented. At least two of the production arc dipole magnets must be mapped to obtain an absolute field integral measurement with an accuracy of 2.5×10^{-4} .

The proposed method requires a beam position measurement with an accuracy of better than 50 μ m. An upgrate CEBAF harp beam profile monitor ("Superharp") [6] is under development. The absolute beam position readout is realized by a multi-turn encoder (COMPUTER CONVERSION CORP. Model no. HTMDS90-64-DB18-1p) which backlashlessly connects the end shaft of stepping motor and provide a parallel binary output with 18 bit resolution. For the beam energy measurement, 6 superharps are required. The basic performance of the "Superharp" is listed below:

Table 17. Specification of Superharp

Material of sensor wire 7 - 10 μ tungsten wire Minimum step size of translation $0.6 \mu m$ (variable) Accuracy of absolute calibration better than $10\mu m$ Repeativity of mechanical travel better than $10\mu m$ Dynamic range of readout 1 - 200 μ A Dynamic range of translation 7.63 cm Observable vibration magnitude less than $3\mu m$ Maximum linear velosity 3.81mm/s (variable) 18 Bit Resolution of the encoder Total number of units 6 \$8,000 Estimate cost for each

Then the beam position can be expressed as the position of center of mass of beam profile:

$$x_{cm} = \frac{\sum_{i} n_{i} x_{i}}{\sum_{i} n_{i}}$$

where x_i and n_i - the position readout and the current readout at i-th step respectively. The accuracy of beam position mainly depends on the precision of translate motion of mechanical driving system.

Now, the first prototype of Superharp is being tested and developed by the collaboration of CEBAF detector group and Hall C group. Instead of directly current readout, Michael Tiefenback used a beam loss monitor (with and without scintillators) to get a secondary emission beam profile which is as good as the current readout. In future, the same technique can be used for beam position measurement at very low current (in the order of few ten nA) by harp (or superharp).

5. Chicane for Polarized Target

The high polarization of the nucleon target is produced when the appropriate target material is irradiated with high frequency microwaves at 1°K in the presence of a strong magnetic field. The UVa polarized target will have a 5 T magnetic field over the active target region with a total Bdl of 2.5 T-m along the axis of the magnet. The bending power of this magnet will require a consideration of the trajectories of the incident beam, the scattered electrons, and any recoil charged particles.

Therefore, a vertical chicane is necessary to transport CEBAF beam to the polarized target as shown in Figure 18. At the entrance of Hall C the incident beam is bended down about 1° by 1m vertical bending magnet BE, and is transported into the second 3 m bending magnet BZ which is placed at 4 m before the target. The beam is vertically deflected by this magnet for about 5° towards the

target. Like a dipole magnet, the 5T magnet (Helmholtz pairs) of polarized target bends the beam in the opposite direction, by about 4° and another 3m bending magnet BZ bends the beam to the beam dump. These bends will have the effect of keeping \vec{q} close enough to horizontal to be acceptable to the HMS and the plane of the neutron detector close enough to horizontal so its placement will not be constrained by the Hall C layout.

Six beam position monitors will be placed in the exit of BE, the entrance of BZ, the both sides of 5T magnet, and the exit of 2-nd BZ to ensure a reliable beam operation. The polarized target chicane will be also used as beam transport system for HNSS which requires a few cm horizontal offset on the target position. In this case only one BE and one BZ bending magnets are used and the chicane works in the horizontal plane. The final geometry was defined on May 26, 1993. In order to calculate the chicane optics a group of parameters is defined as:

| $l_1 = 453.06 \text{ cm}$ | distance between centers of target and BZ_1 |
|-----------------------------|--|
| $l_2 = 1352.84 \text{ cm}$ | distance between centers of BE and BZ_2 |
| $l_3 = 1352.84 \text{ cm}$ | distance between centers of target and BZ ₂ |
| $l_4 = 2253.94 \text{ cm}$ | distance between center of BZ_2 and 6 m before beam dump |
| $L_{eff} = 54.4 \text{ cm}$ | effective length of Oxford magnet |
| $L_1 = 1 \text{ m}$ | effective length of BE |
| $L_2 = 2 \text{ m}$ | effective length of BZ_1 |
| $L_3 = 2 \text{ m}$ | effective length of BZ_2 |
| ϕ_{\circ} | deflection by Oxford 5 T magnet |
| ϕ_1 | deflection by BE magnet |
| ϕ_2 | deflection by BZ_1 magnet |
| ϕ_3 | deflection by BZ_2 magnet |
| ϕ_4 | the angle from BZ_2 to 6 m in front of dump |
| h_1 | vertical offset of BZ_1 |
| h_{2} | vertical offset of BZ_2 |

Table 18. Specifications of Chicane Magnets

| Element | BE | 1-st BZ | 2-nd BZ |
|------------------------------|---------|---------|---------|
| Location to target in cm | -1805.9 | -453.06 | 453.06 |
| Effective Length in cm | 100.0 | 200.0 | 200.0 |
| Gap in cm | 2.54 | 3.81 | 3.81 |
| Pole Width in cm | 11.8 | 27.9 | 27.9 |
| Max. \int Bdl in Tm | 1.0 | 2.0 | 2.0 |
| DC Resistance in Ω | 0.055 | 0.079 | 0.079 |
| Field Setting in kG | 4.48 | 9.05 | 8.15 |
| Driving Current in A | 228 | 306 | 276 |
| Max. Power Dissipation in kW | 2.859 | 7.397 | 6.017 |

Table 19. Operational Parameters of Chicane

| E_{\circ} | $\phi_{\circ}(^{\circ})$ | $h_1(cm)$ | $\phi_{\scriptscriptstyle 1}(^{\circ})$ | $\phi_{\mathbf{a}}(^{\circ})$ | $\phi_3(°)$ | $\phi_4(^{\circ})$ | $B_{i}(kG)$ | $B_2(kG)$ | $B_3(kG)$ |
|-------------|--------------------------|-----------|---|-------------------------------|-------------|--------------------|-------------|-----------|-----------|
| 1.0 | 23.5257 | 191.317 | 8.0493 | 31.5750 | 4.8517 | 28.3774 | 4.6863 | 9.1915 | 8.2607 |
| 2.0 | 11.7007 | 91.013 | 3.8488 | 15.5495 | 2.3123 | 14.0130 | 4.4815 | 9.0529 | 8.1584 |
| 3.0 | 7.7929 | 60.243 | 2.5455 | 10.3384 | 1.5285 | 9.3214 | 4.4460 | 9.0285 | 8.1404 |
| 4.0 | 5.8427 | 44.970 | 1.9039 | 7.7466 | 1.1430 | 6.9857 | 4.4338 | 9.0201 | 8.1341 |
| 5.0 | 4.6735 | 35.925 | 1.5211 | 6.1946 | 0.9131 | 5.5866 | 4.4279 | 9.0162 | 8.1313 |
| 6.0 | 3.8942 | 29.915 | 1.2668 | 5.1609 | 0.7604 | 4.6546 | 4.4252 | 9.0140 | 8.1297 |

6. Beam Raster System

6.1 Heating effect in the solid target

Assume that a beam current is 200 μ A and the target periphery is kept fixed at the initial target temperature 20 K. The beam spot size is about 0.2 mm diameter. A thin molybdenum target of 2×2 cm² is considered. The target thickness is 0.2 mm, which corresponds to about 0.15% radiation length (0.204 g/cm²) for molybdenum. In this case thermal conduction the each the metal target material and the metal frame is considered as the major mains of releasing the heat deposited by the beam. With eliminating the blackbody thermal radiation the steady state beam spot temperature reachs 2500 K when the beam spot is fixed at the center of the target. If the beam scans the target with a sinusoidal motion having frequency 100 Hz and amplitude 9.6 mm in one direction, the steady temperature is about $300 \, \, \mathrm{K}$ over the target area except the four vertex points of the motion [7]. A further simulation by [8] shows that if a fast two dimensional rastering $(f_1 = 2 \text{ kHz and } f_2 = 0.1176 \text{ kHz})$ is applied to an aluminium target (20 mm × 20 mm), the temperature distribution on the target will be quickly saturated after 1 second exposure to 200 μ A electron beam. The temperature rise Δt is below 70 K at an initial temperature 300 K. For the iron target a temperature rise of 500 K occurs due to the worse termal conductivity and the smaller specific heat.

6.2 Heating effect in the cryogenic target

In the case of a 10 cm liquid hydrogen target operating at 20 K the power dissipation due to the energy loss in the target cell by 200 μ A beam is about 1 kW. The liquid hydrogen is overheated by the depossited beam energy and bubbles are formed, therefore, a density variation is eventually generated. In order to minimize this bubble formation effect and reduce forced flow velocity to a reasonable level (1 to 10 m/s), the best solution is beam rastering. The global and local beam heating analysis by [9] shows a 18 kHz rastering with 2 mm amplitude is preferable.

6.3 Heating effect in the beam dump

As discussed by [10], for an instantaneous spot size of 100 μ m, the critical time constant for drilling a hole into the window is 100 μ s. Also, any window material loses its strength after an energy deposition of 10¹⁸ ergs/gram by the beam. Therefore, the rastering speed and pattern have to be selected carefully to avoid long dwell times. Tentatively, a spot size of 4×4 cm² at the dump was adopted. The spot size at the beam dump entrance can be increased nearly arbitrarily by using high speed magnetic rastering.

6.4 Rastering on the polarized target

The polarized target will have a useful width and height of 2.5 cm. To make full use of it, the rastering of the beam on the target should cover at least 2.5×2.5 cm² [11]. An adjustable offset of rastering current is desirable for the beam alignment. In the polarized target experiment the current density is only 100 nA; it is reasonable to require 1 kHz rastering. The Moller polarimeter requires a linear rastering pattern on the iron target with amplitude of 2 mm instead of moving the target [12]. The linear scan of the beam will effectively reduce the temperature rise of the target and keep the polarization at a higher level in the beam current range from 10 to 100 μ A.

Table 20. gives rastering parameters required by different target materials.

Table 20. Raster frequency and amplitude, FR: fast raster, SR: slow raster

| Parameter | Cryogenic | Polarized | Polarimeter | Beam Dump |
|------------------|------------------|------------------|-------------|------------|
| | Target | Targt | Iron Target | Materials |
| $L_{target}(m)$ | 141.6 | 141.6 | 101.6 | 188.6 |
| $L_{raster}(m)$ | 121.1 | 121.1 - 122.2 | 52.25 | 139.6 |
| $Current(\mu A)$ | 200 | 0.1 | 0.05 - 100 | 200 |
| Area (cm2) | 0.2×0.2 | 2.5×2.5 | linear 0.2 | 4×4 |
| Frequency(kHz) | 10-18 | 0.1-1 | 0.1 | 0.1 |
| Operation | FR | FR+SR | FR | SR |

6-5. Raster Magnet Design by TOSCA

Two bedstead air core coils are used as the raster magnets. Based on TOSCA calculation, the specifications of these coils are listed in Table 2.

Table 21. Specification of SR and FR magnets

| Design Parameter | SR | FR |
|--------------------------------------|-----------------------|-----------------------|
| Central field (Gauss) | 438.8 | 80.1 |
| Bending angle at 6 GeV | 0.84 mr | 0.0588 |
| $\int Bdl$ (kG cm) | 16.8 | 1.2 |
| Field uniformity | 10-2 | 10-2 |
| Effective length (cm) | 38.34 | 15 |
| Physical dimension (cm) | 48 | 25 |
| Inner radius (cm) | 1.905 | 1.27 |
| Number of turns | 200 | 20 |
| Ampere-turns (A-T) | 4000 | 240 |
| Current density (A/cm ²) | 148 | 100 |
| Stored energy (Joules) | 6.944 | 0.0167 |
| Inductance (H) | 34.7×10^{-3} | 84×10^{-6} |
| DC resistance (Ω) | 0.916 | 3.02×10^{-3} |
| RMS power (kW) | 2.18 | 0.528 |
| Type of conductors | Awg 8 | Litz |
| Rastering frequency (Hz) | 60 | 10,000 |

The geometry of the raster magnet is shown in Figure 19. The bedstead shape of the raster coil will generate a larger uniform field region and keep the high order field components, mainly the sextupole component, as small as possible. In order to reach a higher rastering frequency up to 10 kHz, neither iron nor laminate iron material can be used as the raster magnet. A ferrite magnet is also not preferable because its small hysteresis makes it difficult for phase control.

A triangle waveform is selected to drive the raster coil. Based on the Fourier theorem, an arbitary function F(x) can be expressed

$$F(x) = \sum_{n=1}^{\infty} [A_n \sin n\omega_n x + B_n \cos n\omega_n x]$$
 (1)

where $\omega_n = 2 \pi f_n$, the amplitude of the n-harmonic is $\sqrt{A_n + B_n}$ and the intensity of the n-harmonic is $A_n^2 + B_n^2$. In the case of an identical triangle waveform

$$y = \begin{cases} -T - x & -T \le x \le -T/2 \\ x & -T/2 \le x \le T/2 \\ T - x & T - x \le x \le T \end{cases}$$
 (2)

the Fourier expension of the triangle waveform is

$$y = \frac{4T}{\pi^2} \sum_{n=1}^{\infty} \frac{(-1)^{n-1}}{(2n-1)^2} \sin \frac{(2n-1)\pi x}{T}$$
 (3)

$$y = \frac{4T}{\pi^2} \left[\sin(\frac{\pi x}{T}) - \frac{1}{9} \sin(\frac{3\pi x}{T}) + \frac{1}{25} \sin(\frac{5\pi x}{T}) - \dots \right]$$
(4)

therefore, the ratios of the amplitudes and the intensities of the first, the third, and the fifth harmonic components are $1:\frac{1}{2}:\frac{1}{2}$ and $1:\frac{1}{8}:\frac{1}{225}$ respectively.

and the fifth harmonic compoenets are $1:\frac{1}{9}:\frac{1}{25}$ and $1:\frac{1}{81}:\frac{1}{225}$ respectively. The 20 kHz triangle waveform generated from the Tektronix FG 501A 2 MHz function generator was experimentally analyzed by an HP network analyser. The frequency spectrum is displayed in Figure 20. The ratio of relative amplitudes of the fundamental frequency and the third and the fifth harmonics is as the same as the computation from Fourier analysis mentioned above. The frequency range of a triangle waveform should cover 3-order harmonic.

Losses in a conductor due to the skin effect and proximity effect should be considered. For the FR magneyt, a round Litz cable 660/36 is used for the winding. For the SR magnet, Litz cable is replaced by awg 6 solid cable because the skin depth in copper conductors is 8.5 mm at lower frequency (60 Hz).

6.6 Operational performance

The Hall C raster system is arranged as shown in Figure 21. A fast raster (FR) system is placed at the entrance of Hall C, just in front of the first chicane magnet (BE). With a bending power 0.0588 mr at 6 GeV it is able to provide 2×2 mm² rastering area on the cryogenic target. A combined SR system which is located in front of the FR scans the beam on the polarized target with rastering area 2.5×2.5 cm². The second SR near the target chamber, executes two functions: in the absence of the polarized target it scans the beam to a safety size $(4 \times 4 \text{ cm}^2)$ on the beam dump, and in the operation of the polarized target, it derasters the beam with opposite phase in order to reduce the large ammount background generated from scattered beam at the beam pipe walls.

Each raster system consists of two pairs of bedstead coils, one for horizontal scan, another for vertical scan. Different rastering patterns have been simulated and compared by two dimensional oscillascopic Lissajous figures. The best ratio (1.721) of the two rastering frequencies was found, which gives the longest trajectory traversal and fast uniform distribution.

The FR magnet is driven by PA03 MOS power amplifier (APEX μ TECHNOLOGY CORPORATION), which has excellent features of high supply voltage (150 V), high output current (30 A), and high internal dissipation (500 W). The SR magnet is driven by a resonance circuit, which consists of a π -type LC resonance circuits, impedance match network, and low frequency power amplifier. Both of those drivers are under development.

A ceramic duct should be used as the vaccum pipe of FR magnet. The ceramic vaccum duct avoids the heating-up effect and the field attenuation due to eddy currents induced by alternating magnetic field. A very thin metal coating layer should be applied in the inner wall of the duct conducting the image current produced by the beam.

References

- [1] C. Yan, R. Carlini, S. Lassiter, J. Napolitano, R. Wines, S. A. Wood, Preliminary User's Manual of High Momentum Spectrometer, January 6, 1991, CEBAF-R-92-002
- [2] C. Yan, D. Neuffer, J. Napolitano, R. Carlini, Beam Energy Measurement for Hall C, January 6, 1991, CEBAF-R-92-001
- [3] D. Neuffer, C. Yan, R. Carlini, Hall C Beam Momentum Measurement System, November 24, 1992, CEBAF-TN-92-054
- [4] R.V. Servranckx, Energy Measurement on Beam Switchyard Line of Hall C September 29, 1992, CEBAF-TN-92-044,
- [5] C. Yan, R. Carlini, J. Napolitano, D. Neuffer, R. Rossmanith, Use Achromatic Beam Line for Hall C Beam Energy Measurement, March 25, 1991, CEBAF-R-92-003
- [6] C.Yan, P. Adderley, R. Carlini, F. Feldl, H. Feng Progress Report on the Superharp, January 16, 1993, CEBAF-TN-93-006
- [7] Conceptual Design Report on Basic Experimental Equipment (revised), CE-BAF, April 13, 1990.
- [8] Javer Gomez, Private communication, December 1992.
- [9] J. Mitchell, Global and Local Beam Heating in the Hall C Cryo Target, CE-BAF, March 2, 1993.
- [10] B. Mecking and C. Sinclair, Memorandum, Meeting on Beam Lines to Experimental Area, 28 November, 1992
- [11] D. Day and I. Sick, Memorandum: Considerations Concerning Chicane for G_{en}, July 23, 1992.
- [12] Matthias Loppacher, Progress Report of the CEBAF Hall C Moller Polarimeter, November 1992.

Frela departent variables:

L, = 1.889 m cet 1.508 Testa

L_3 = 2.186 cm cet 1.5293 Testa

L_3 = 2.186 cm cet 0.3321 Testa

Ly = 5.2519 m cet 1.563 Testa

Li - Ly effective lengths

and physical aperture

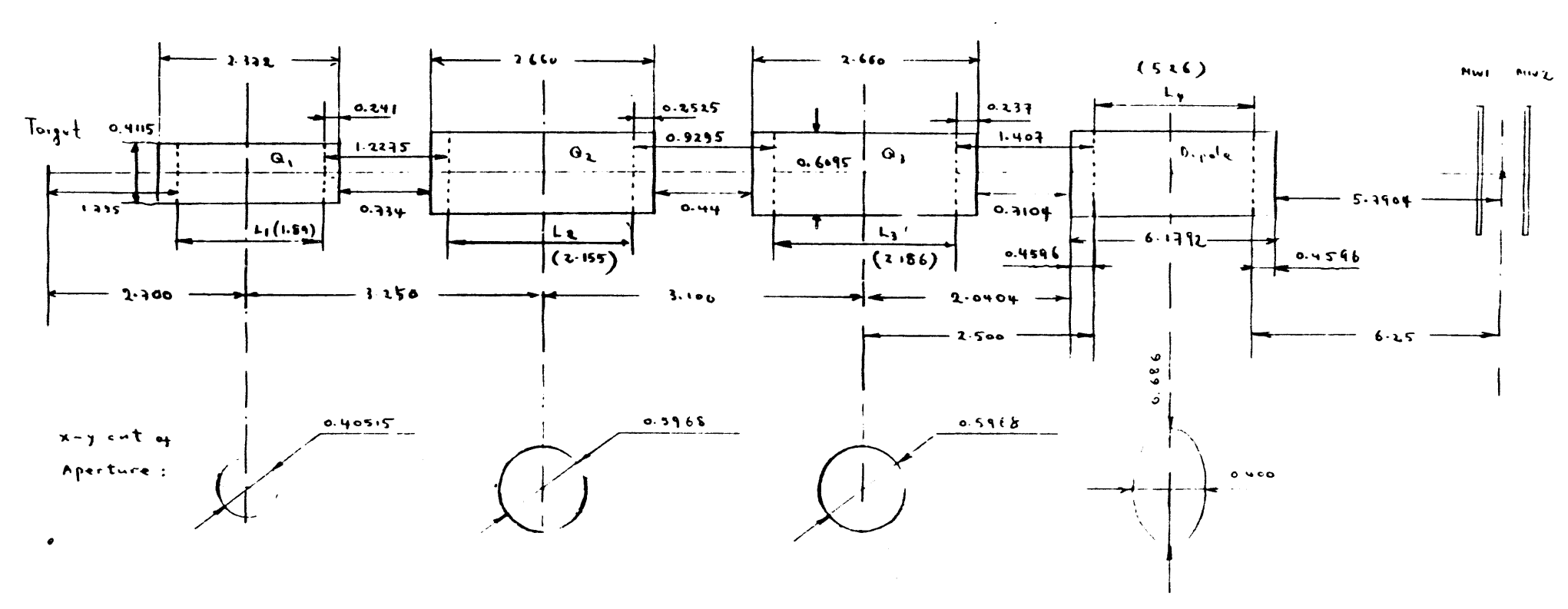


Figure 1. Layout of HMS physical aperture

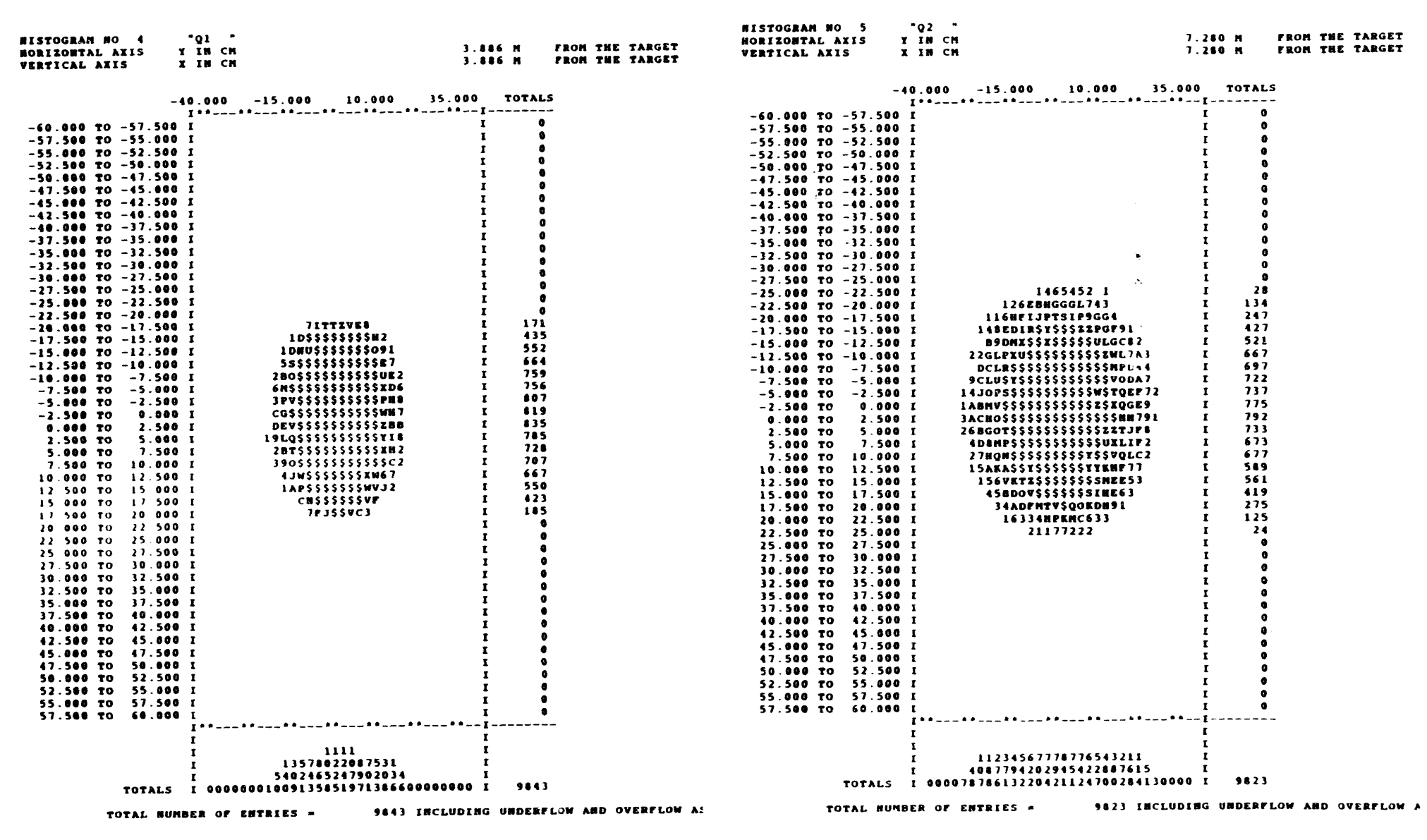


Figure 2-1. Histogram display of beam envelope after the first quadrupole from TURTLE in HMS-1 focusing mode (point-to-point).

Figure 2-2. Histogram display of beam envelope after the second quadrupole from TURTLE in HMS-1 focusing mode (point-to-point).

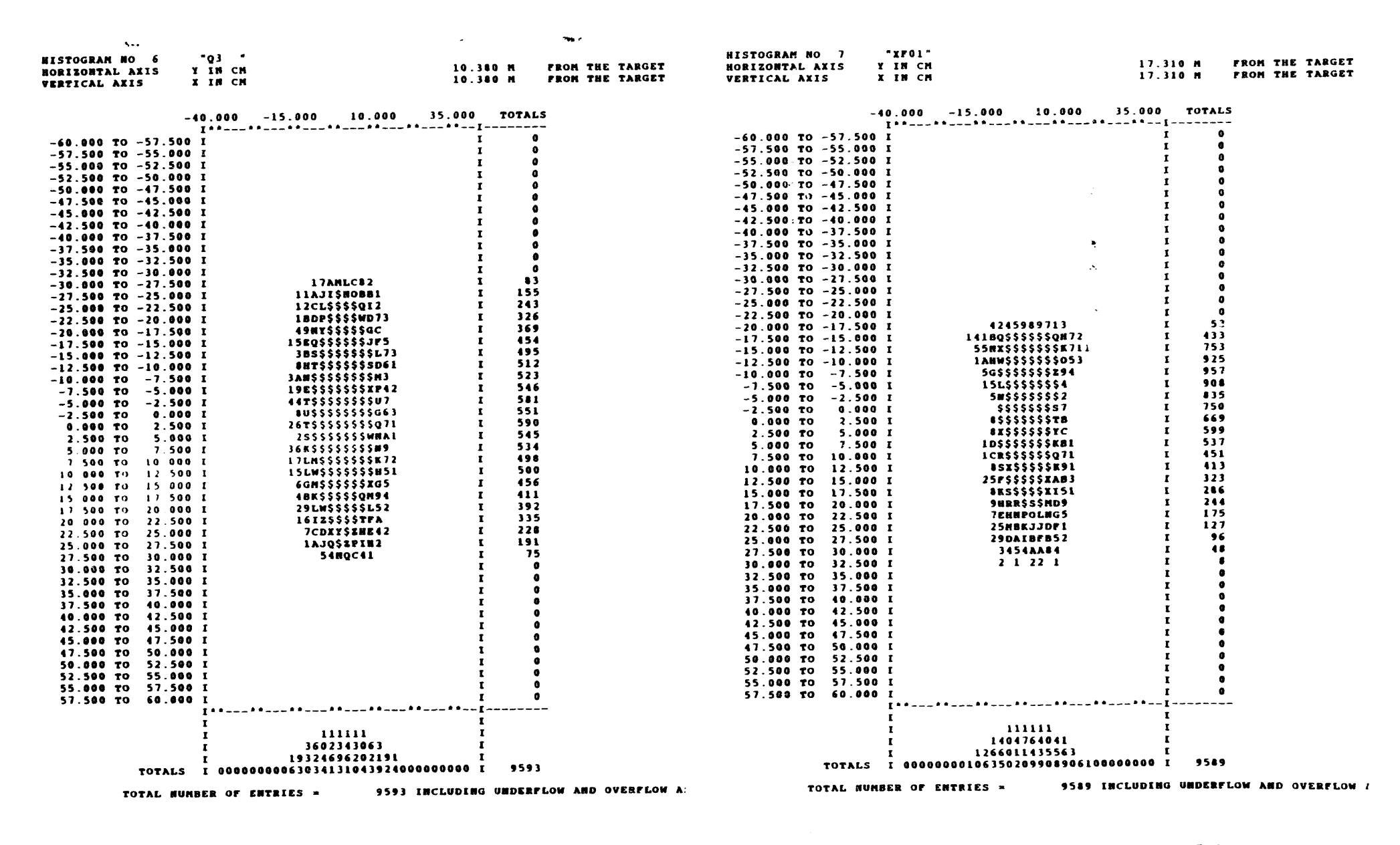


Figure 2-3. Histogram display of beam envelope after the third quadrupole from TURTLE in HMS-1 focusing mode (point-to-point).

Figure 2-4. Histogram display of beam envelope after the dipole magnet from TURTLE in HMS-1 focusing mode (point-to-point).

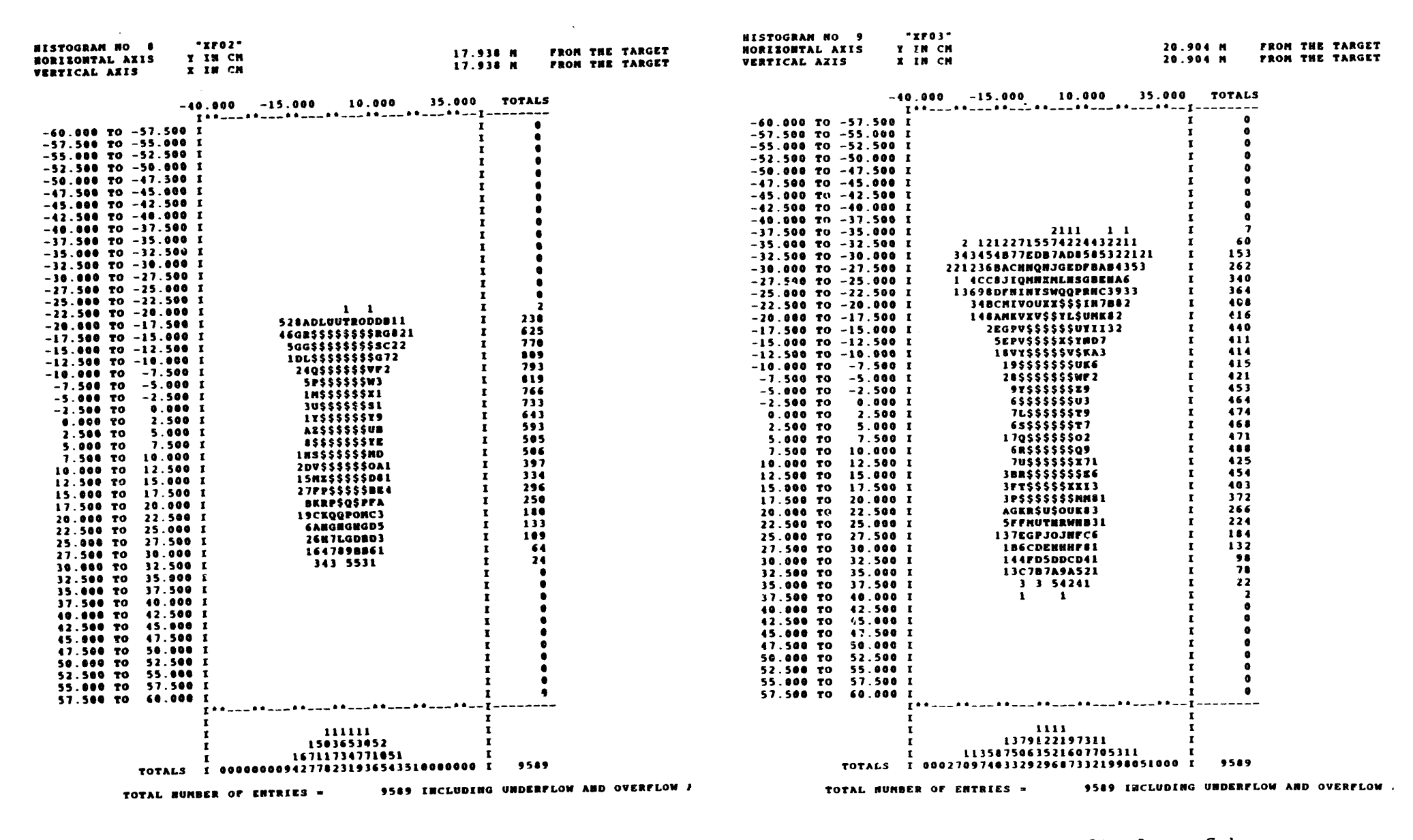


Figure 2-5. Histogram display of beam envelope 0.628 m after the dipole magnet from TURTLE in HMS-1 focusing mode (point-to-point).

11.14

Figure 2-6. Histogram display of beam envelope 3.594 m after the dipole magnet from TURTLE in HMS-1 focusing mode (point-to-point).

"NW1 " HISTOGRAM NO 11 23.060 M FROM THE TARGET "XF04" HISTOGRAM NO 10 HORIZONTAL AXIS Y IN CH 22.060 M FROM THE TARGET FROM THE TARGET 23.060 M A IN CM VERTICAL AXIS X IN CH MORIZONTAL AXIS 22.060 H FROM THE TARGET X IN CM VERTICAL AXIS -40.000 -15.000 10.000 35.000 TOTALS -40.000 -15.000 10.000 35.000 TOTALS -60.000 to -57.500 I -57.500 TO -55.000 I -60.000 TO -57.500 I -55.000 TO -52.500 I -57.500 TO -55.000 I -52.500 TO -50.000 I 11 -55.000 TO -52.590 I 1 123211211 2 121 -56.000 TO -47.500 I -52.500 TO -50.000 I 11 12 3 25251225213 24 1 11 47 -47.580 TO -45.000 I -50.000 TO -47.500 I -47.500 TO -45.000 I -45.000 TO -42.500 I 2 333535454142334232351 1 1 1122 11 1 1 -45.000 TO -42.500 I -42.500 TO -40.000 I 213111363367CA735B394433412 111 I 121 1 3 42224443 113113 1 40 163 -42.500 TO -40.000 I -40.200 TO -37.500 I 2122212854889DG8CA855556431311 I 22 333564A524245434531 1 1 -37.500 TO -35.000 I 2 1572378406DG7F568E94528331211 I -40.000 TO -37.500 I 179 21332252474FC96A95C4473231 11 139 -35.000 TO -32.500 I 11437577A9FEFHGEFGC9FCA6962 1 264 -37.500 TO -35.000 I 12111643F88F7LJDDB6A968631512 286 -32.500 TO -30.000 I 21766859BFLFQEKIBE8D6737522 -35.000 TO -32.500 I 245 -30.000 TO -27.500 I 311 2484659ERMMEN6BHCCA2D45 2 11 12578IIGJGJLDIROMIA96471 -32.500 TO -30.000 I 325 23599AFDEKGITHLVDEJB967521 -27.500 TO -25.000 I 234378CCENFGQNMEENJ6874322 -30.000 TO -27.500 I 2 1176CGIFLHOLKLEPIB74921 304 282 -25.000 TO -22.500 I 344789BHGIGOMPHHAF8AA342 -27.500 to -25.000 I 1355DEGHEFPQSESTQBD66541 357 4A5FDHHVIROMFLHHEA532 319 -25.000 TO -22.500 I -22.500 TO -20.000 I 334 25698GMETLTQUEGJJIM44 313 -22.500 TO -20.000 I -20.000 TO -17.500 I 1 37F8KIPMVSORLHFA9813 2A9IJOSRYSSSPOOBA34 -20.000 TO -17.500 I -17.500 TO -15.000 I 19AHTWORZXKHJFFF64 334 361 -17.500 TO -15.000 I 13EHO#\$\$\$ZPSRMWA5 1 -15.000 TO -12.500 I 143DLUKSHXSHHKFF51 305 351 25PH\$TYE\$YPWEE55 -12.500 TO -10.000 I 28IOUP\$TPUXDMD32 317 -15.000 TO -12.500 I 14GRTQ\$W\$\$WQKJ51 360 15ATIRUZVQR\$KE74 323 -12.500 TO -10.000 I -10.000 TO -7.500 I 17LU\$\$\$VP\$UM94 352 25KGKXXVWSTFE5 283 -7.500 TO -5.000 I -10.000 TO -7.500 I 15KSWSSSSSXMAL 353 AQS\$\$\$Z\$URM6 355 -5.000 TO -2.500 I -7.500 to -5.000 I 1KTSSSSSSXW1 383 5DS\$\$\$Y\$YVP3 341 -2.500 TO 0.000 T -5.000 TO -2.500 I 390 E2SSSSSSWD IMSSSSSSSD -2.500 TO 0.000 I 0.000 TO 2.500 I 394 340 0 000 TO 2.500 I ESSSSSSSW9 2.500 TO 5.000 I 1DXZSXSSSP8 175555555IM1 402 195\$\$\$\$\$\$**ZUM**4 5.000 TO 7.500 I 2.500 TO 5.000 I 408 389 16555555XX8 7.500 TO 10.000 I 39X\$\$\$\$\$\$TBL 7.500 I 5.000 TO 438 190\$\$\$\$\$\$P81 10.000 TO 12.500 E AR\$\$\$\$\$WKA1 362 10.000 I 7 500 TO 388 8#\$\$\$\$\$\$T8 12.500 TO 18GU\$\$\$\$\$OA1 331 12.500 I 10.000 TO 378\$\$\$\$\$\$172 381 3DEU\$\$\$\$\$TC21 376 15.000 TO 17.500 I 12.500 TO 15.000 I 410 370 17.500 I 2GG\$\$\$\$\$W\$F5 17.500 TO 29.000 I 3GL\$\$\$\$\$\$UD51 15.000 TO 4AV\$\$\$\$\$\$\$ 399 26.000 TO 22.500 I 69P\$\$\$\$\$YED61 350 17.500 TO 20.000 I 369 40USSSSSWRLA 22.500 TO 25.000 I 37HV\$\$\$\$W\$5#61 22.500 I 20.000 TO 293 38MEJSTTTQWM71 303 2 THEYWYHOLOLE L 25.000 TO 27.500 I 22.500 TO 17GHQJWQPOL86 26GMWPVHLTKI9 27.500 TO 30.000 I 25.000 TO 27.500 I 181 37CGLLJMOLFE73 200 30.000 I 25BDMJFHK#BK62 36.000 TO 32.500 I 27.500 TO 476DCGIRMO56 32.500 TO 35.000 I 1 666DCCGMGR85 145 30.000 TO 32.500 I 110 109 248MA6DFDE7L 35.000 TO 37.500 I 25AFC4DHDC42 35.000 1 32 500 TO 22A698A89322 37.500 TO 237777A75633 67 40.000 I 35.000 TO 37.500 T 20 21212322 15 12 313334 40.000 TO 42.500 I 37.500 TO 40.000 I 42.500 TO 45.000 I 40.600 TO 42.500 I 45.000 TO 47.500 I 42.500 TO 45.000 I 47.500 TO 50.000 45.000 TO 47.500 I 50.000 TO 52.500 I 47.500 TO 50.000 I 52.500 TO 55.000 I 50.000 TO 52.500 55.000 TO 57.500 I 52 500 TO 55.000 I 57.500 57.500 TO 60.000 I 55.808 TO 57 588 TO 60.000 I 1124689009874211 1133604399887366097407442 12469011096421 114471139254051944284421 TOTALS I 26759960053853735983533407119742 I TOTALS I 01482924180777947518800186214410 I 9589 TOTAL NUMBER OF ENTRIES = 9589 INCLUDING UNDERFLOW AND OVERFLOW i SER THEIRDING SUBDERFLOW AND OVERFLOW TOTAL MINERS OF PRINTERS -

Figure 2-7. Histogram display of beam envelope 4.75 m after the dipole magnet from TURTLE in HMS-1 focusing mode (point-to-point).

Figure 2-8. Histogram display of beam envelope at the first wire chamber from TURTLE in HMS-1 focusing mode (point-to-point).

| | HW2 * | .060 M PROM THE TARGET | | Ql " In ch 3 | .886 M FROM THE TARG |
|--|---|--|--|--|----------------------|
| | | .060 M FROM THE TARGET .060 M FROM THE TARGET | | IN CH 3 | .886 H FROM THE TARG |
| -40 | .000 -15.000 10.000 35.00 | ę totals | | | 0 TOTALS |
| | **********- | | - | ******** | -I |
| 60.600 TO -57.500 I | | I 0 | -60.000 TO -57.500 I -57.500 TO -55.000 I | | i o |
| 57.500 TO -55.000 I | | I 17 | -55.000 TO -52.500 I | | ī 0 |
| 55.000 TO -52.500 I | | I 34 I 40 | -52.500 TO -50.000 I | | I 0 |
| 12.506 TO -50.000 I | 111 311 133122 2111 41233 1 1 1 12343233542423741621332 2 | 1 73 | -50.000 TO -47.500 I | | I 0 |
| 17 500 TO -47.309 I | 211111236242AAB44385353341311 1 | - | -47.500 TO -45.000 I | | I 0 |
| 5.000 TO -42.500 I | | I 124 | -45.000 T) -42.500 I | | 1 0 |
| 2.500 TO -40.000 I | 2172 4664C1A98B656B55242331242 | I 144 | -42.500 TO -40.000 I -40.000 TO -37.500 I | | 1 0 |
| 0.000 TO -37.500 I | 224646676A86EKAB8676DAA36622 | I 201 | -37.500 TO -35.000 I | | i o |
| 7.500 TO -35.000 I | 2122425796AC8DAHGEFSAA8494953211 | I 244 I 241 | -35.000 TO -32.500 I | | I 0 |
| 15.000 TO ~32.500 I | 11145417B7CFE8G99GGFC99A43A411 1 3387DEFD9GGMFEMGGDEB35221 | 1 270 | -32.500 TO -30.000 I | | I 0 |
| 12.300 TO -30.000 I | 114138687BFAFIMMLJCGI778543211 | 1 276 | -30.000 TO -27.500 I | | I 0 |
| 7.500 TO -25.000 I | | I 234 | -27.500 TO -25.000 I | | 1 0 |
| 5.000 TO -22.500 I | 47587DGGLJMOKCAGHHHA341 | I 289 | -25.000 TO -22.500 I -22.500 TO -20.000 I | | T 0 |
| 2.500 TO -20.000 I | | I 278 | ~20.000 TO -17.500 I | 4 HWU S Y P 7 | Î 182 |
| 0.000 TO -17.500 I | | I 292 I 290 | -17.500 TO -15.000 I | 1 EX\$\$\$\$\$\$M | I 445 |
| 7.506 TO -15.600 I | | 1 265 | -15.000 TO -12.500 I | 12125\$\$\$\$\$991 | I 545 |
| 5.600 TO -12.500 I 2.500 TO -10.000 I | | 1 296 | -12.500 TO -10.000 I | 34\$\$\$\$\$\$\$\$65 | I 660 |
| 0.000 TO -7.500 I | | I 278 | -10.000 TO -7.500 I | 2A#\$\$\$\$\$\$\$\$WC1 | I 759 |
| 7.500 TO -5.000 I | | I 274 | -7.500 TO -5.000 I | 5K\$\$\$\$\$\$\$\$UE4 | I 738 I 803 |
| 5.000 TO -2.500 I | 3ETM\$S\$MUROED1 | I 314 | -5.600 TO -2.500 I -2.500 TO 0.000 I | 71M\$\$\$\$\$\$\$\$\$00E 612\$\$\$\$\$\$\$\$\$\$6 | I 810 |
| 2.500 TO 0.000 I | | I 267 | 0.000 TO 2.500 I | | I 827 |
| 0.000 TO 2.500 I | | I 322 I 302 | 2.500 TO 5.000 I | | 1 774 |
| 2.500 TO 5.000 I 5.000 TO 7.500 I | | 1 319 | 5.000 TO 7.500 I | 2BU\$\$\$\$\$\$\$\$\$WM2 | I 719 |
| 5.000 TO 7.500 I 7.500 TO 10.000 I | | 1 347 | 7.500 TO 10.000 I | | I 695 |
| 0.000 TO 12.500 I | | I 337 | 10.000 TO 12.500 I | | I 655 |
| 2.500 TO 15.000 I | | I 313 | 12.500 TO 15.000 I | 18P\$\$\$\$\$\$WRI3 | I 553 I 432 |
| 5.000 TO 17.500 I | | I 326 | 15.000 TO 17.500 I 17.500 TO 20.000 I | | 1 212 |
| 7.500 TO 20.000 I | | I 331 I 330 | 20.000 TO 22.500 I | *************************************** | I 0 |
| 0.000 TO 22.500 I | | I 307 | 22.500 TO 25.000 I | | I 0 |
| 2.500 TO 25.000 I 5.000 TO 27.500 I | | 1 327 | 25.000 TO 27.500 I | | 1 0 |
| 7.500 TO 30.000 I | | I 289 | 27.500 TO 30.000 I | | I 0 |
| 0.000 TO 32.500 I | | I 277 | 30.000, TO 32.500 I | | I 0 |
| 2.500 TO 35.000 I | 47LCTEQESOPD65 | I 237 | 32.50: TO 35.000 I 35.00" TO 37.500 I | | T 0 |
| 5.000 TO 37.500 I | | I 165 | 37.50 TO 40.000 I | | ī |
| 7.500 TO 48.000 I | | I 110 I 63 | 40 80 TO 42.500 I | | r 0 |
| 0.000 TO 42.500 I | | 1 11 | 42.52 TO 45.000 I | | 1 0 |
| 2.500 TO 45.000 I 5.000 TO 47.500 I | | i i | 45 ປມສູ 70 47.500 I | | Ι 0 |
| 7.500 TO 50.000 I | | ī | 47.500° TO 50.000 I | | I 0 |
| 0.000 TO 52.500 I | | r • | 50.000 to 52.500 I | | I V |
| 2.500 TO 55.000 I | | <u>r</u> • | 52.50\$ TO 55.000 I 55.000 TO 57.500 I | | r o |
| 5.000 TO 57.500 I | | I I | 57.500 TO 60.000 I | | ī 0 |
| 7.500 TO 60.000 I | | 1 V | | | -I |
| I | | I | Ī | | T. |
| Ť | | Ī | I | | ī |
| i | 1125649999875311 | I | I. | | I. |
| 1 | 1113357169257476120018195432 | t | I TOTALS I | 4300366248910033 0000000035986589719060391000000 | 1 1 9409 |
| TOTALS I | 70287354994214235601025945581883 | I 9580 | TUTALS I | 4444444124609441144444444 | . ,, |

Figure 2-9. Histogram display of beam envelope at the second wire chamber from TURTLE in HMS-1 focusing mode (point-to-point).

Figure 3-1. Histogram display of beam envelope after the first quadrupole from TURTLE in HMS-2 focusing mode (parallel-to-point).

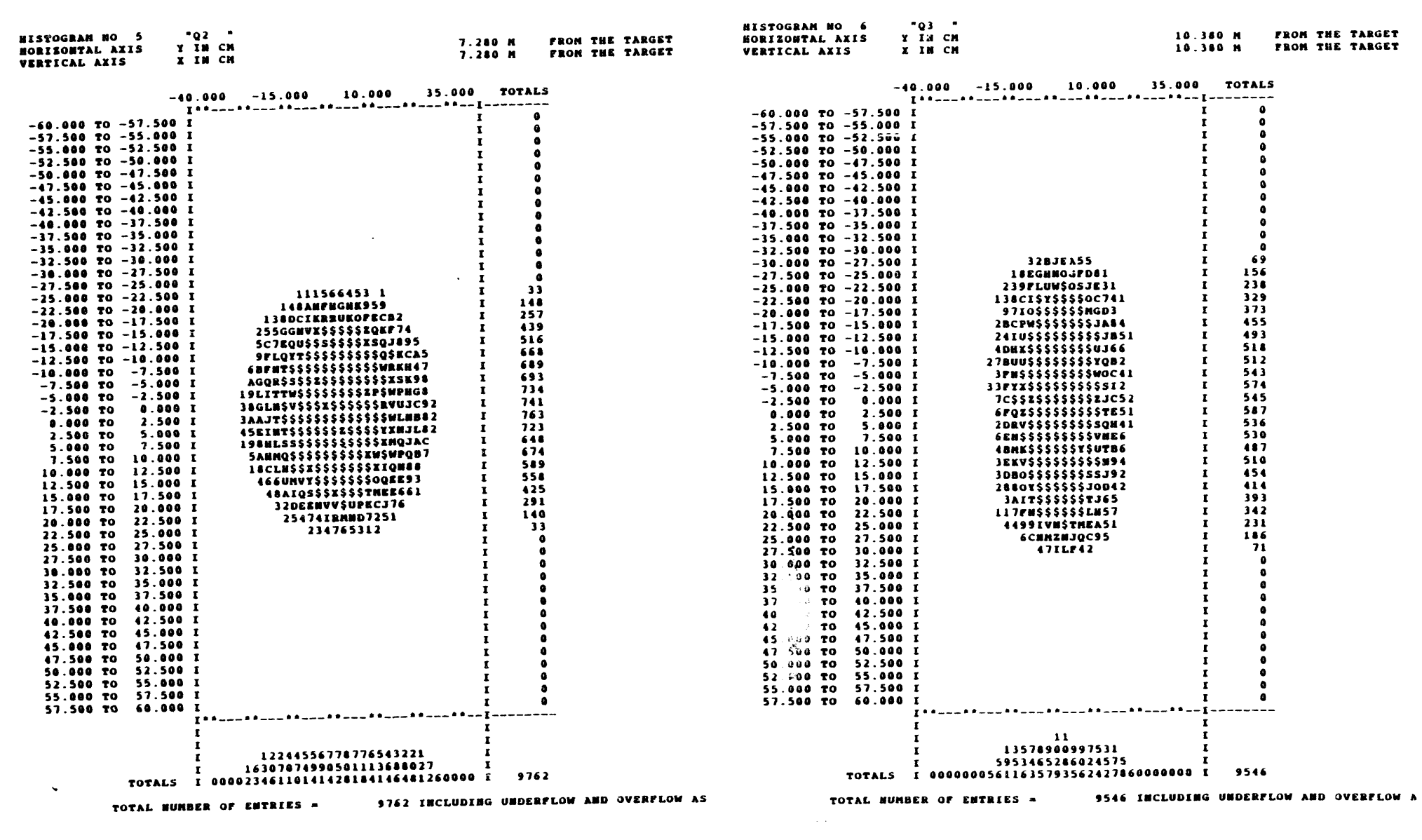


Figure 3-2. Histogram display of beam envelope after the second quadrupole from TURTLE in HMS-2 focusing mode (parallel-to-point).

Figure 3-3. Histogram display of beam envelope after the third quadrupole from TURTLE in HMS-2 focusing mode (parallel-to-point).

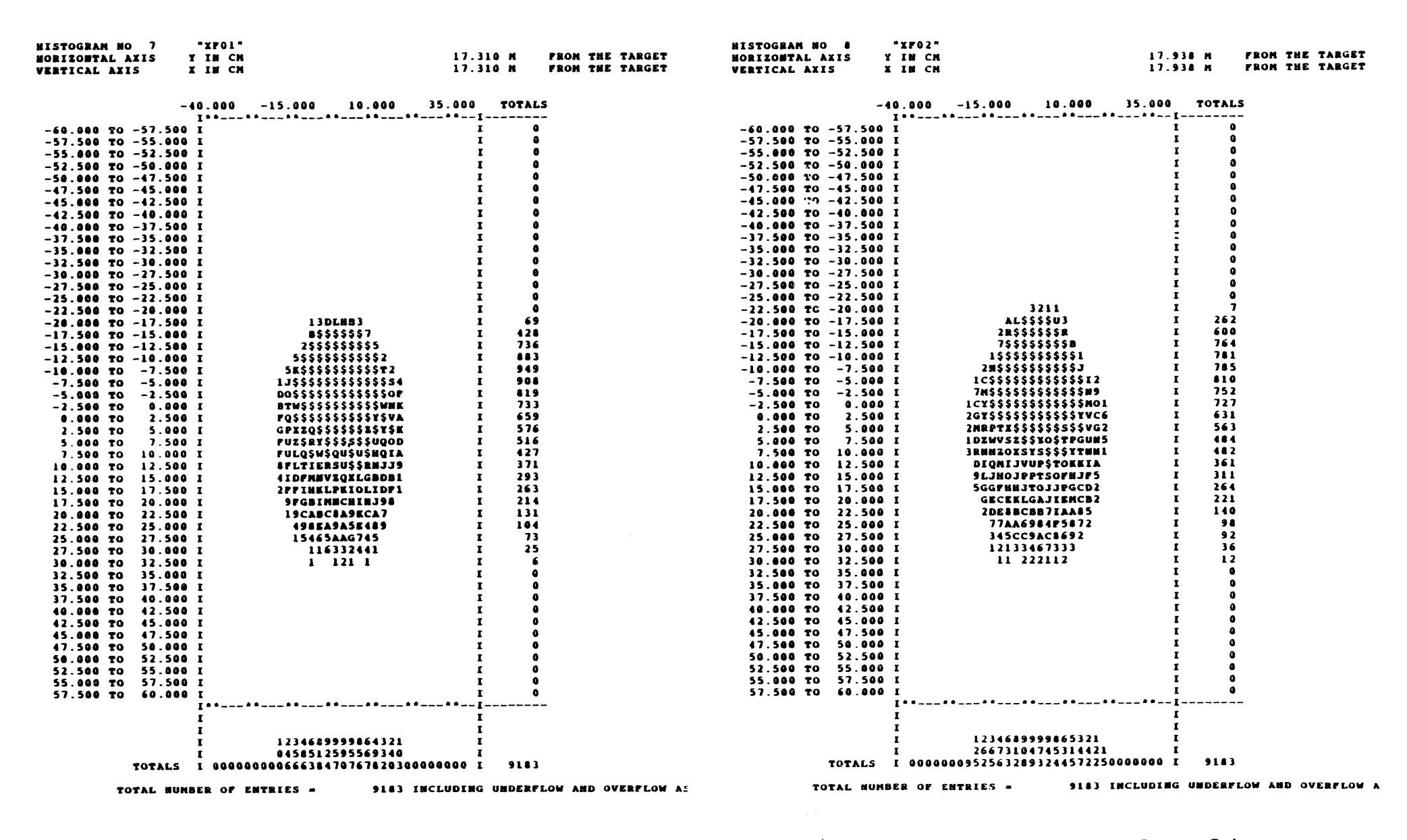


Figure 3-4. Histogram display of beam envelope after the dipole magnet from TURTLE in HMS-2 focusing mode (parallel-to-point).

Figure 3-5. Histogram display of beam envelope 0.628 m after the dipole magnet from TURTLE in HMS-2 focusing mode (parallel-to-point).

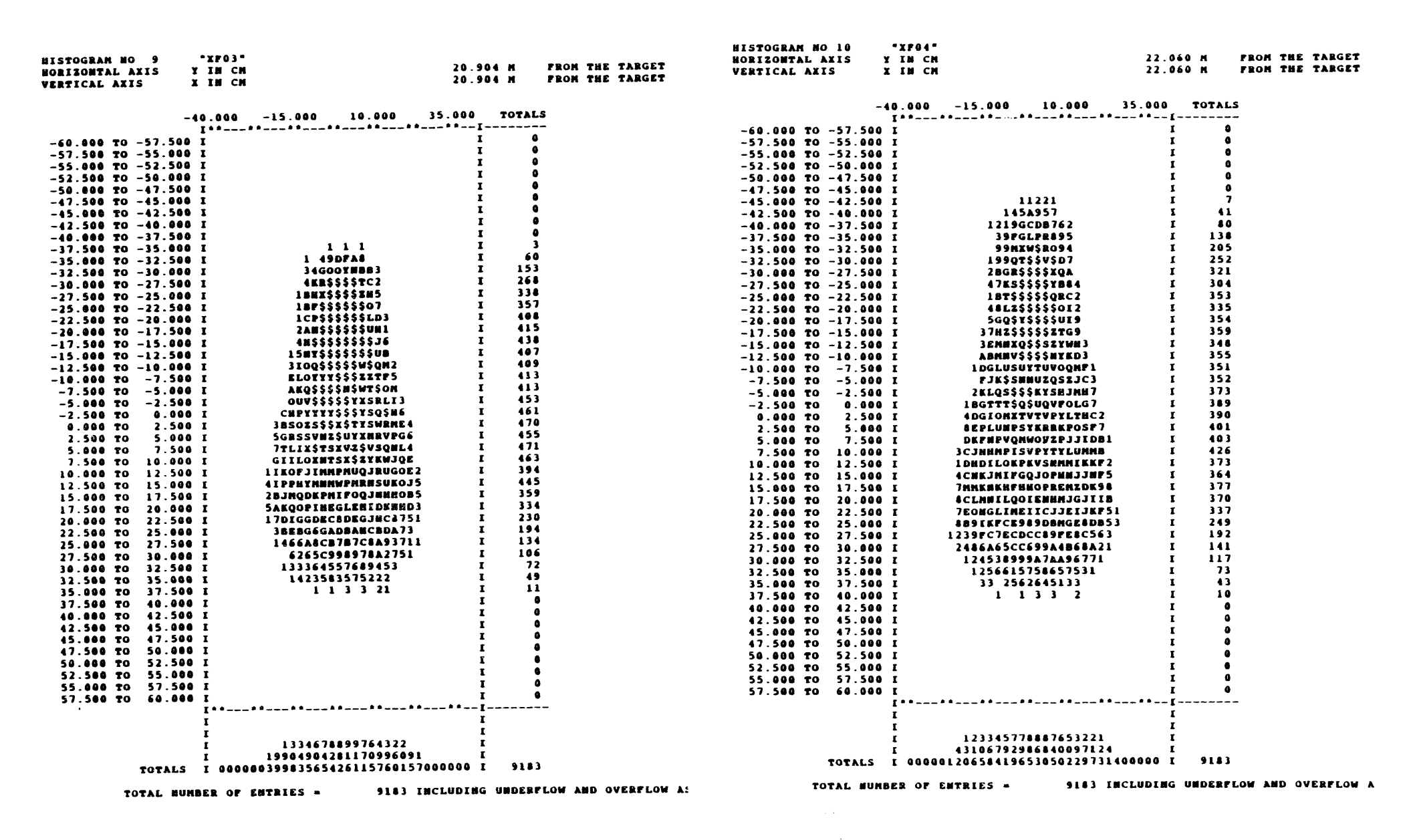


Figure 3-6. Histogram display of beam envelope 3.594 m after the dipole magnet from TURTLE in HMS-2 focusing mode (parallel-to-point).

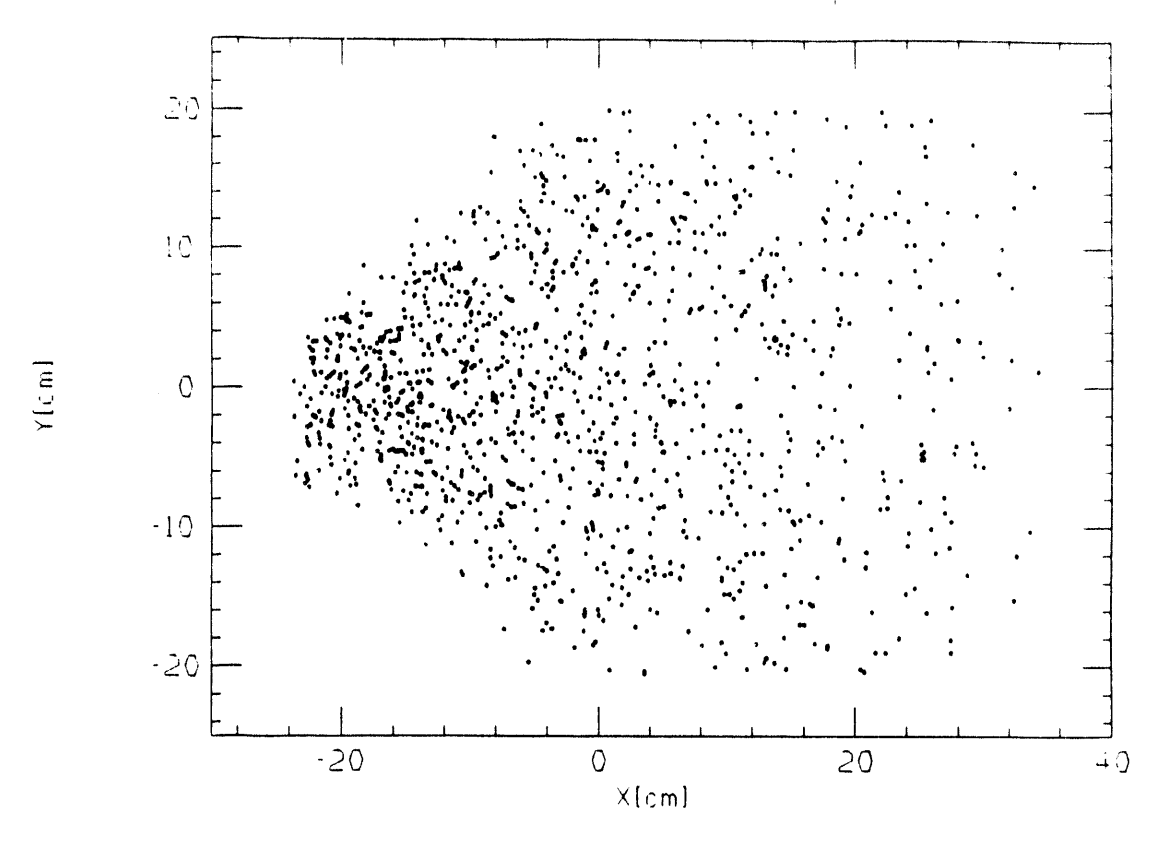
Figure 3-7. Histogram display of beam envelope 4.75 m after the dipole magnet from TURTLE in HMS-2 focusing mode (parallel-to-point).

| | IN CM 'MWl " | 23.060 M FROM THE TARGET | | | 060 M FROM THE TAI |
|--|---|--------------------------|--|--|--------------------|
| | IN CM | 23.060 M FROM THE TARGET | VERTICAL AXIS | CIN CH 24. | 060 M PROM THE TAI |
| | | | | 10.000 -15.000 10.000 35.000 | TOTALS |
| -40 |).000 -15.000 10.000 35. | 800 TOTALS | | I************ | |
| 1.000 TO -57.500 I | | ī 0 | -60.000 TO -57.500 | | I 0 |
| 7.500 TO -55.000 I | | I 0 | -57.500 TO -55.000 | TO T | r 17 r 33 |
| 5.000 TO -52.500 I | | I 0 I 2 | -55.000 TO -52.500 -52.500 TO -50.000 | - - | I 36 |
| 2.500 TO -50.000 I | | i 22 | -50.000 TO -47.500 | | 1 75 |
|).000 TO -47.500 I !.500 TO -45.000 I | | I 44 | -47.500 TO -45.000 | | I 105 |
| .000 TO -42.500 I | • | I 74 | -45.000 Yes -42.500 | | I 131 I 145 |
| .500 TO -40.000 I | 67IEDEN/A2L | I 120 | -42.500 TO -46.000 -40.000 TO -37.500 | | 1 201 |
| .000 TO -37.500 I | | I 164 I 179 | -37.590 TO -35.000 | | I 241 |
| .500 TO -35.000 I | | 1 260 | -35.000 TO -32.500 | | 1 245 |
| 5.000 TO -32.500 I 2.500 TO -30.000 I | | I 262 | -32.500 TO -30.000 | | I 268 |
| .000 TO -27.500 1 | 3A#\$\$\$\$#E86 | I 315 | -30,000 TO -27.500 | | I 273 I 232 |
| .500 TO -25.000 1 | [38QP\$\$\$\$UMA31 | I 286 | -27.500 TO -25.000 -25.000 TO -22.500 | | I 290 |
| .000 TO -22.500 I | 49.44\$.4544 | I 280 I 321 | -23.500 TO -22.500 | | I 274 |
| .500 TO -20.000 1 | | 1 306 | -20.000 TO -17.500 | | I 293 |
| .000 TO -17.500 1 | | 1 333 | -17.500 TO -15.000 | | I 282 |
| .000 TO -13.000 I | | г 299 | -15.000 TO -12.500 | | 1 267 |
| .500 TO -10.000 1 | - | r 314 | -12.500 TO -10.000 | = | [294 [278 |
| .000 TO -7.500 1 | I 58FERQRUQTV##GA5 | I 318 I 277 | -10.000 TO -7.500 -7.500 TO -5.000 | | 1 271 |
| .500 TO -5.000 1 | | t 277 r 353 | -5.000 TO -2.500 | | I 309 |
| .000 TO -2.500 1 | | 1 344 | -2.500 TO 0.000 | | 1 287 |
| 2.500 TO 0.000 I | | 1 346 | 0.000 TO 2.500 | • | I 316 |
| .500 TO 5.000 | | I 334 | 2.500 TO 5.000 | | I 303 I 318 |
| .000 TO 7.500 | | I 360 | 5.000 TO 7.500 7.500 TO 10.000 | | I 318 I 342 |
| .500 TO 10.000 1 | | r 367 r 342 | 10.400 TO 12.500 | | 1 322 |
| .000 TO 12.500 | | 1 329 | 12.500 TO 15.000 | | 1 307 |
| .500 TO 15.000 1 | | 1 355 | 15.800 TO 17.500 | I 6JB4JCK71KLMKPJFCND6 | 1 311 |
| .900 TO 17.500 1 | | I 337 | 17.500 TO 20.000 | | I 314 |
| .000 TO 22.500 | I 39EQFJIDJM9PMHDIDEMG92 | I 316 | 20.000 TO 22.500 | • | I 304 I 284 |
| .500 TO 25.000 | I JEHLJEJUMPHPBHPMBEH92 | I 319 | 22.500 TO 25.000 25.000 TO 27.500 | | 1 205 |
| .000 TO 27.500 | | r 272 r 205 | 27.500 TO 30.000 | | I 262 |
| .500 TO 30.000 | | I 164 | 30.000 TO 32.500 | I 4776EA9MPCB5CAAIAMB9941 | 1 228 |
| .000 TO 32.500 .500 TO 35.000 | | 1 100 | 32.500 TO 35.000 | | 193 |
| .000 TO 37.500 | 1 5356 8367849431 | I 73 | 35.000 TO 37.500 | | I 130 I 73 |
| .500 TO 40.000 | I 4112452544 351 | I 41 | 37.500 TO 40.000 40.400 TO 42.500 | | I 73 I 36 |
| .000 TO 42.500 | | I 6 I 0 | 42.500 TO 45.000 | | 1 4 |
| .500 TO 45.000 | | i 0 | 45.000 TO 47.500 | | I 0 |
| 5.000 TO 47.500 7.500 TO 50.000 | | Ī • | 47.500 to 50.000 | | I • |
| .000 TO 52.500 | | r 0 | 50.806 TO 52.500 | | i 9 |
| .500 TO 55.000 | | I 0 | 52,500 TO 55.000 55.000 TO 57.500 | | i 0 |
| 5.000 TO 57.500 | | 1 U | 57.500 TO 60.000 | | ī ē |
| 7.500 TO 60.000 | I | * * I | 222 | I********** | [|
| | 1 | ī | | r | I |
| | ï | I | | 1 | I |
| | 1 122345778867653221 | ī | | I 123345678887553321 I 2882076996040281811682 | I T |
| | 1 1644985918344300991561 | I 000 I 9183 | TOTALS | 1 00001506619396250490903186820000 | 9183 |
| TOTALS | I 00000128284725545744233300400 | AAA . | | | |

Figure 3-8. Histogram display of beam envelope at the first wire chamber from TURTLE in HMS-2 focusing mode (parallel-to-point).

Figure 3-9. Histogram display of beam envelope at the second wire chamber from TURTLE in HMS-2 focusing mode (parallel-to-point).

20% beam. 45cm after dipole



30% beam. At First WC

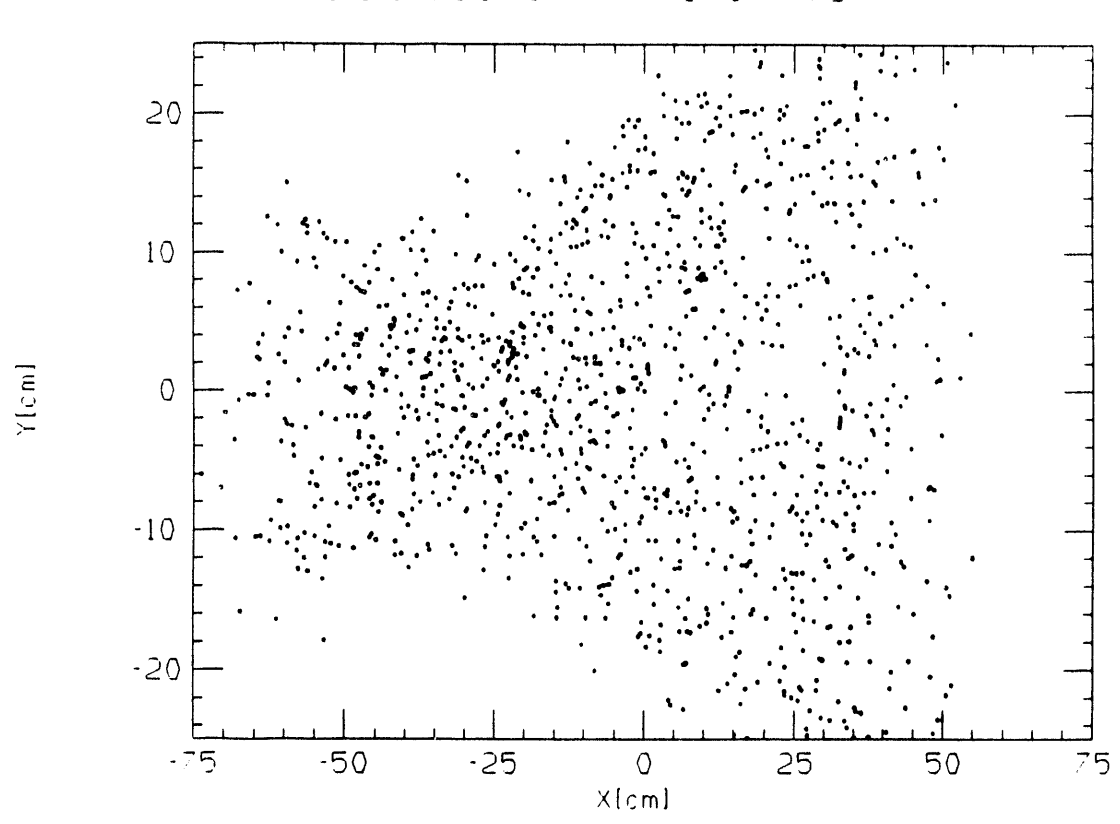


Figure 3-10. Beam envelope displayed by MOTER for HMS-2 at the first and second wire chambers.

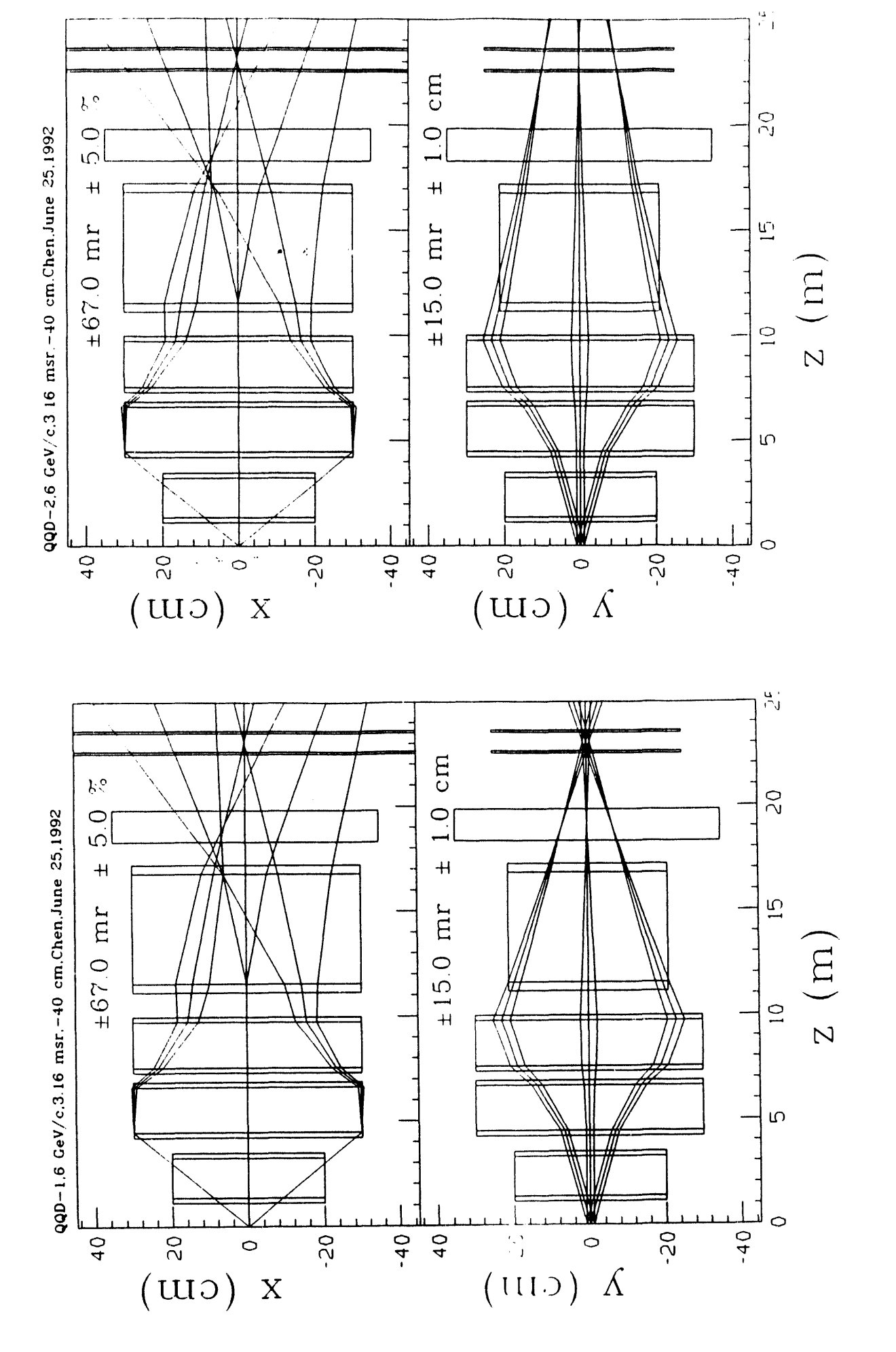


Figure 5. The beam envelope through HMS in QQD-2 (shut down Q1, parallel-to-point mode)

Figure 4. The beam envelope through HMS in QQD-1 (shut down Q1, point-to-point mode)

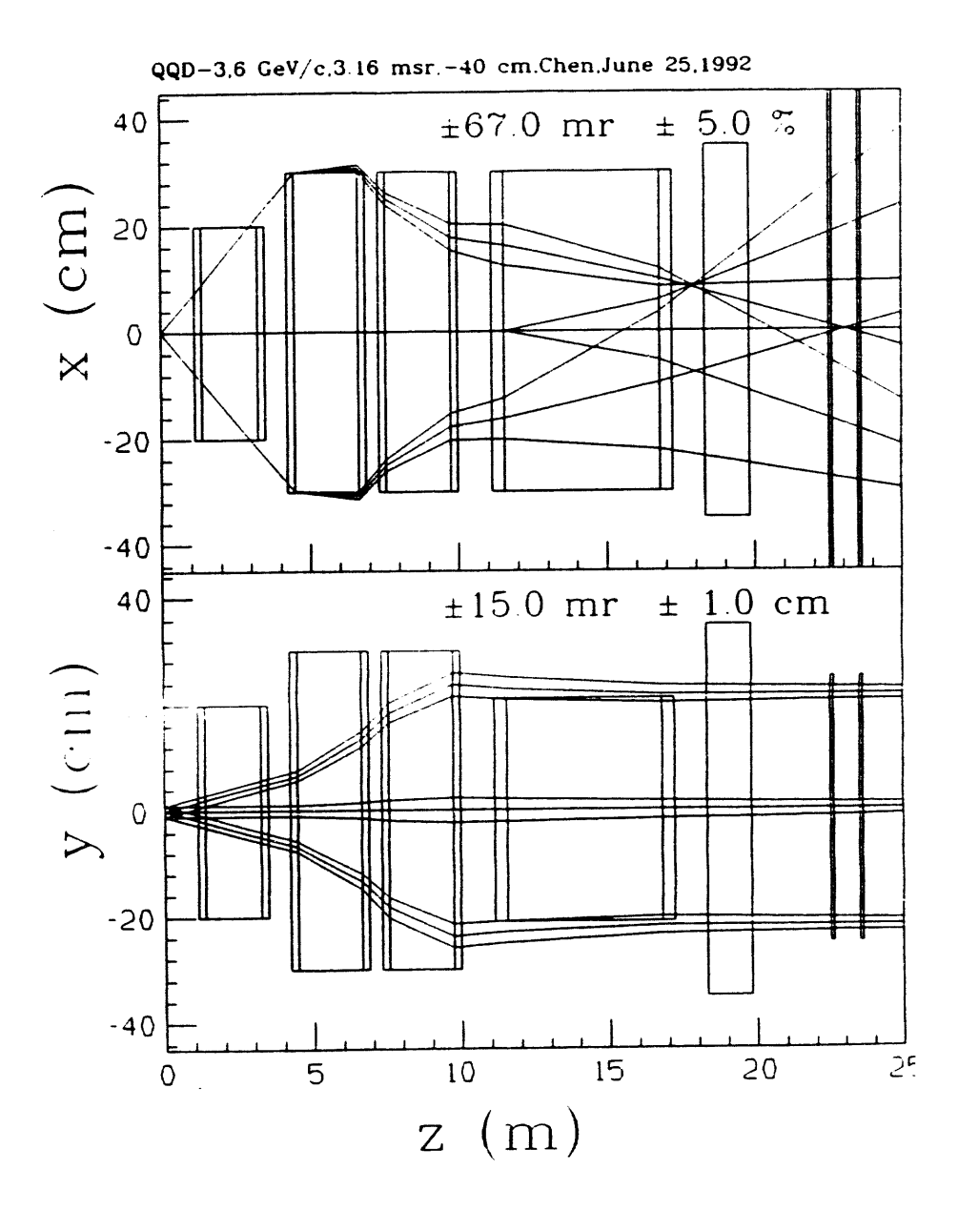


Figure 6. The beam envelope through HMS in QQD-3 (shut down Q1, point-to-parallel mode)

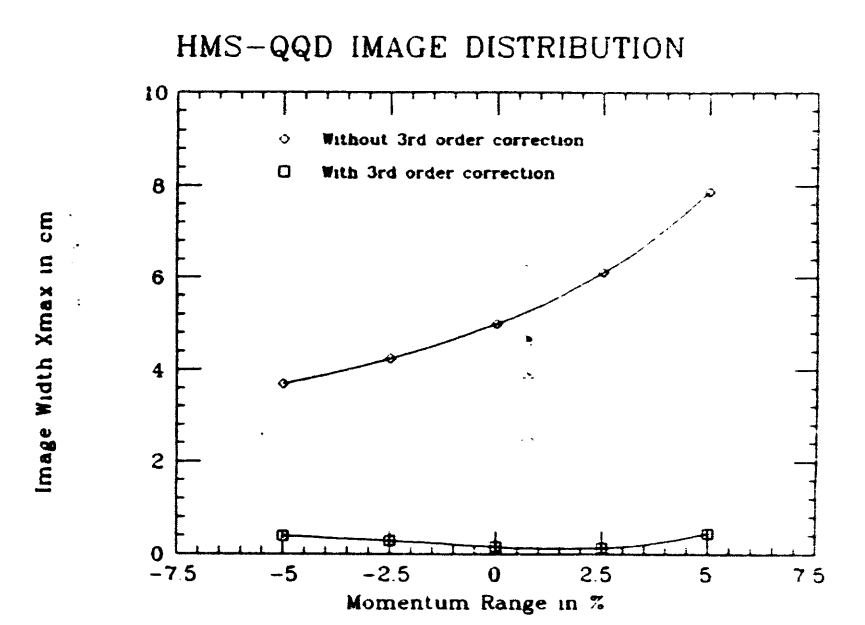


Figure 7. Image behaviour along the focal plane in QQD mode. The main contribution to image widths comes from the 3-rd order aberrations. With a proper 3-rd correction QQD can also keep a resolution better than 10E-3 over 10% momentum range.

| | THWL T | |
|--------------------|---|-----------------|
| HORIZONTAL AXIS Y | IN CM 23.060 M | FROM THE TARGET |
| VERTICAL AXIS X | IN CM 23.060 M | FROM THE TARGET |
| | | |
| | | |
| -4 | | 0 TOTALS |
| | [* - | |
| -60.000 TO -55.000 | | 0 |
| -55.000 TO -50.000 | | 0 |
| -50.000 TO -45.000 | | 0 |
| -45.000 TO -40.000 | | 0 |
| -40,000 TO -35.000 | | 0 |
| -35.000 TO -30.000 | | 568 |
| -30.000 TO -25.000 | | 3058 |
| -25.000 TO -20.000 | | 6022 |
| -20.000 TO -15.000 | | #6L3 |
| -15.000 TO -10.000 | I 9R\$ | 9999 |
| ~10.000 TO ~5.000 | I 177555555555555555555555555555 | 9999 |
| -5.000 TO 0.000 | | |
| 0.000 TO 5.000 | I 7K\$ | 9999 |
| 5.000 TO 10.000 | I 4K\$ | 8848 |
| 10.000 TO 15.000 | I 29x55555555555555555555 | 7408 |
| 15.000 TO 20.000 | | 6057 |
| 20.000 TO 25.000 | | 4611 |
| 25.000 TO 30.000 | | 3203 |
| 10.000 TO 35.000 | | 2049 |
| 15.000 TO 40.000 | | 1044 |
| 40.000 TO 45.000 | | |
| 45.000 TO 50.000 | | 0 |
| 50.000 TO 55.000 | | ŏ |
| | i i | Ŏ |
| | [* [| |
| | i | |
| | 1 112334556666655433211 1 | |
| | I 1483952851604454150581584841 I | |
| | 1 486547601302058357764590947994 1 | |
| TOTALS | 1 0000251209909695100803090860061414400000 1 | 97482 |

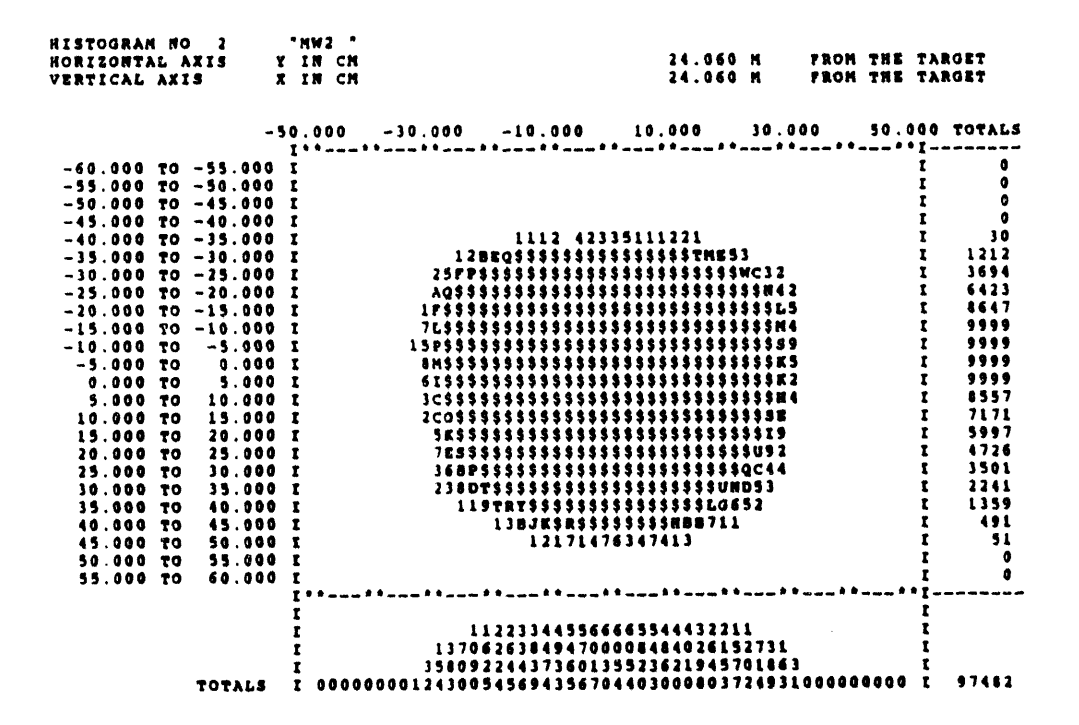


Figure 8-1. Beam envelope at the first and second wire chambers for HMS with alternate quadrupole polarities from TURTLE.

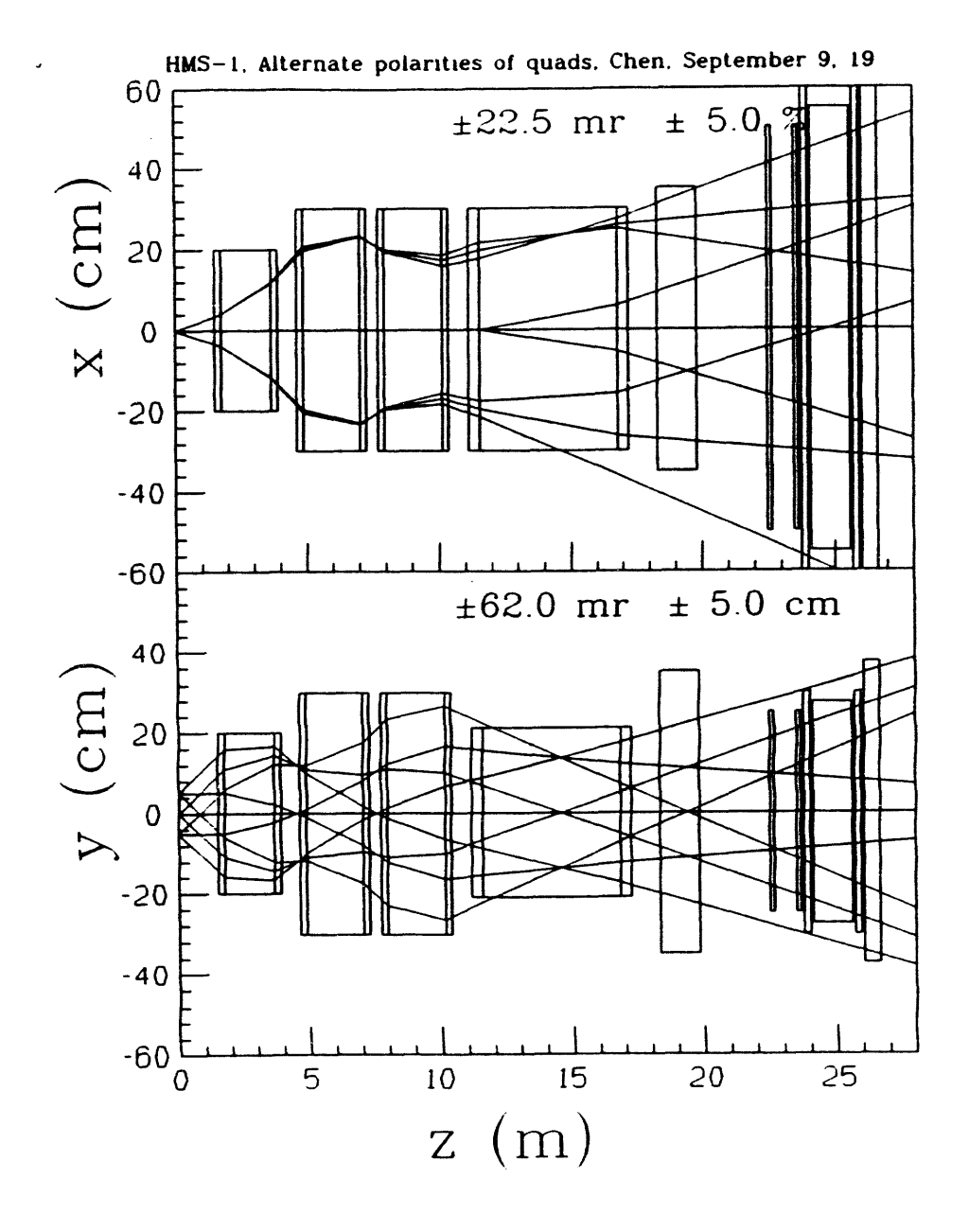


Figure 8-2. Beam envelope along the central axies for HMS with alternate quadrupole polarities from TRANSPORT.

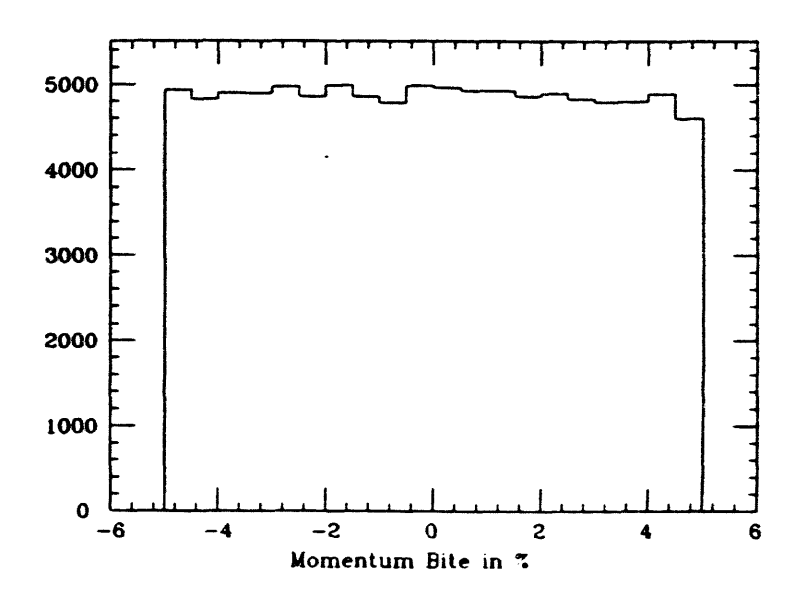


Figure 9. Momentum acceptance for HMS with alternate quadrupole polarities from TURTLE.

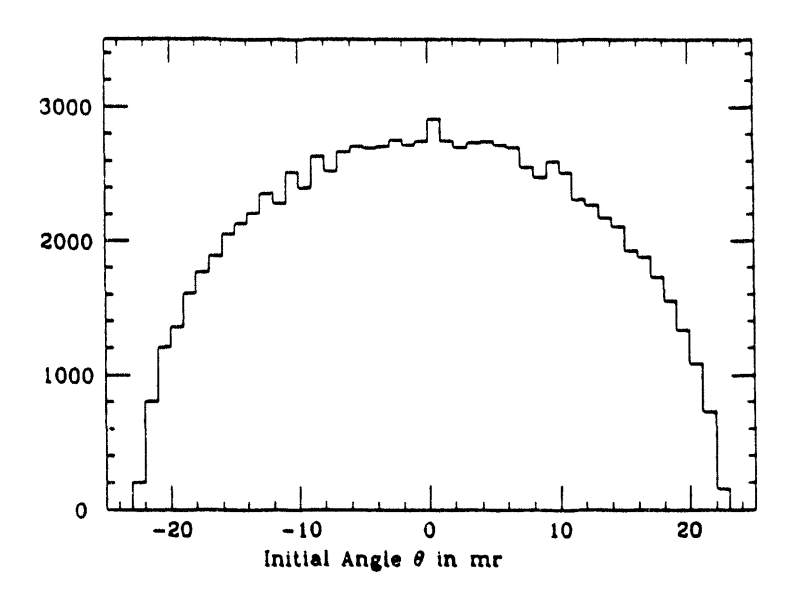


Figure 10. Geometric acceptance (incident angle) for HMS with alternate quadrupole possiss from TURTLE.

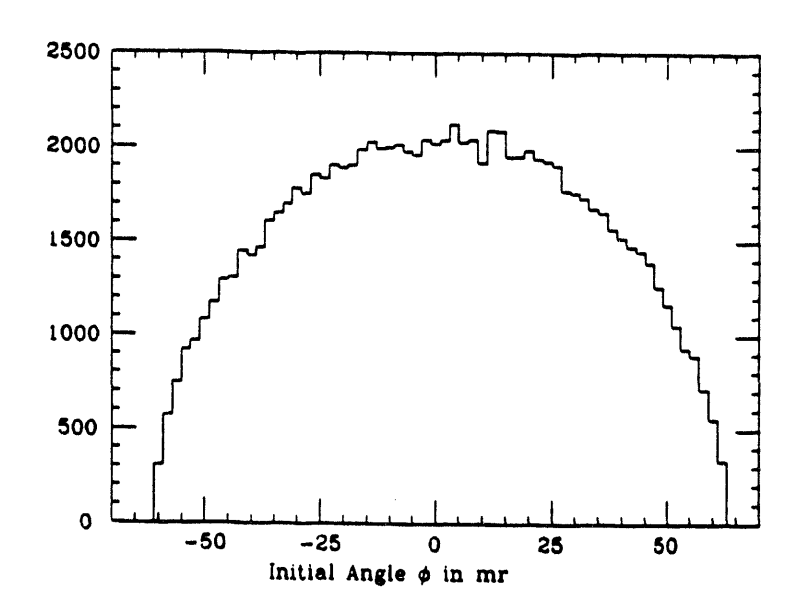


Figure 11. Geometric acceptance (scattering angle) for HMS with alternate quadrupole polarities from TURTLE.

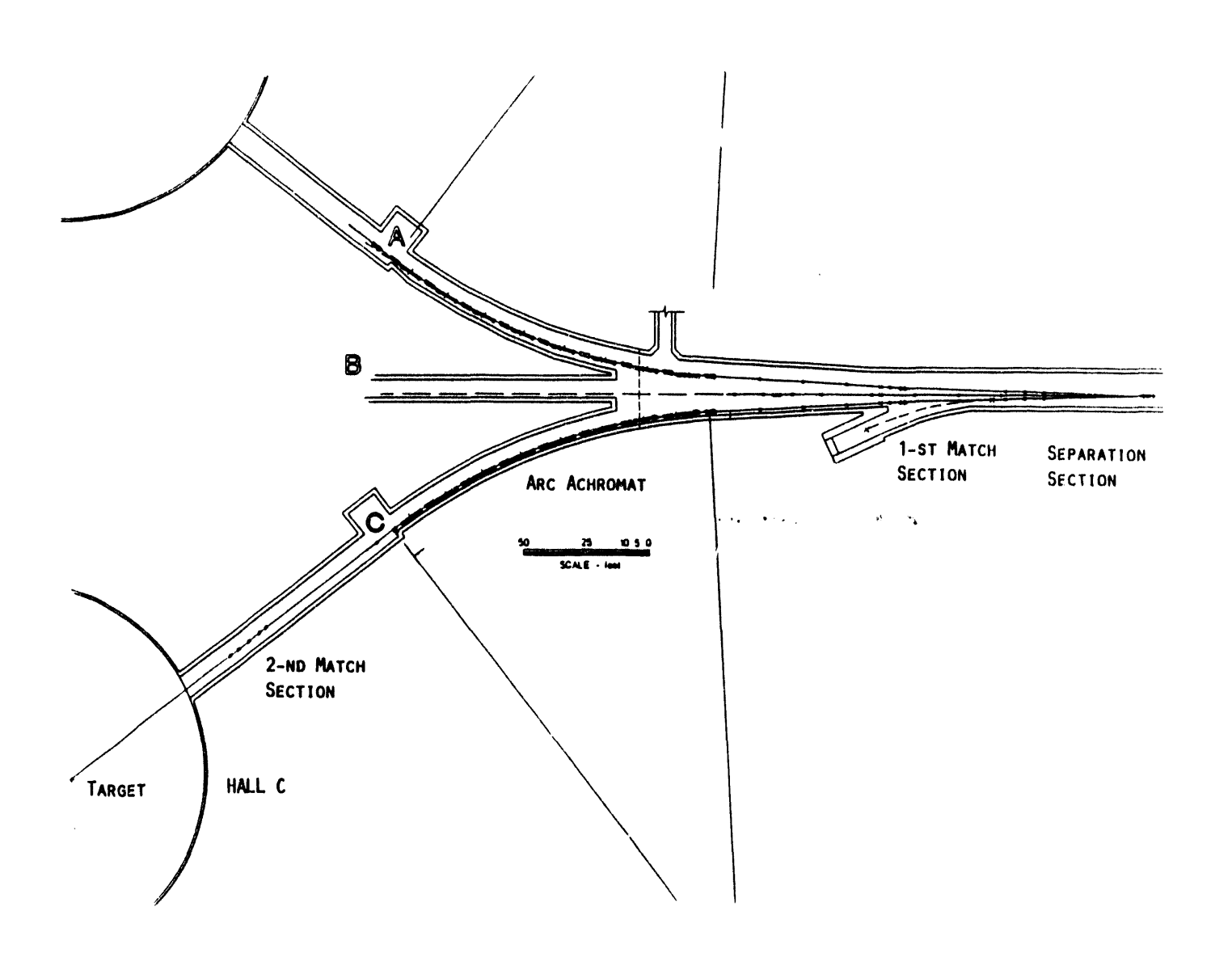


Figure 12. Layout of Hall C beam line

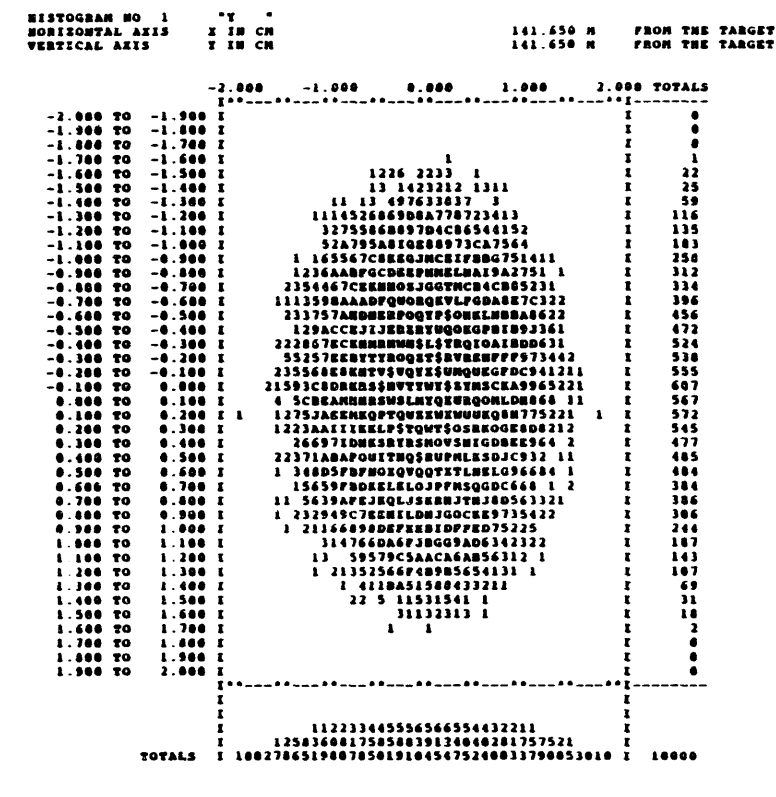


Figure 13. The histogram of beam spot on the polarized target. The beam is defocused to 2.5x2.5 cm2 by the quadrupole cluster in the second match section.

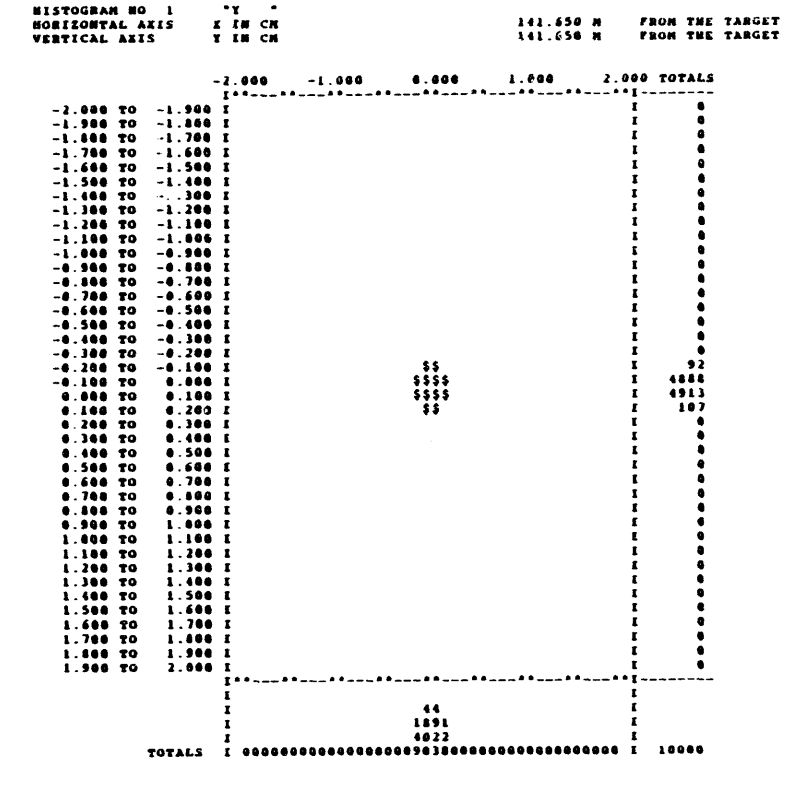
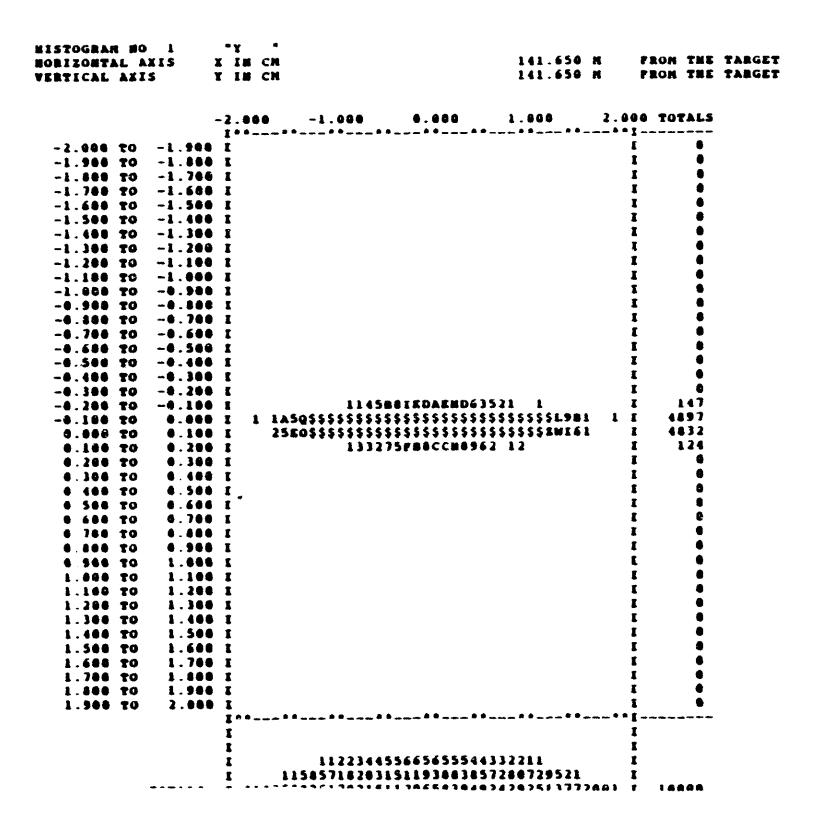
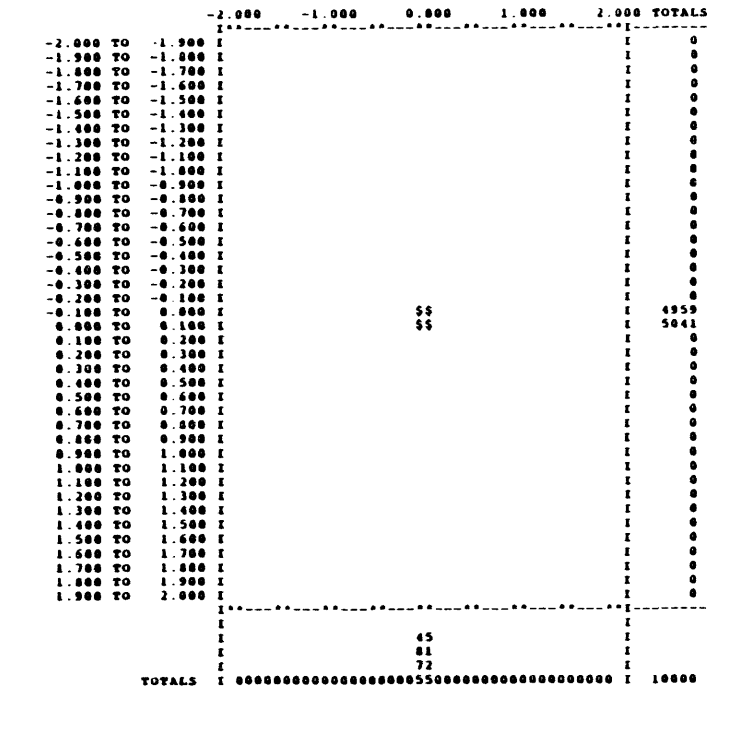


Figure 14. The histogram of beam spot on the cryogenic target. The beam is defocused to 0.1x0.1 cm2 by the quadrupole cluster in the second match section.





141.650 M

FROM THE TARGET

MISTOGRAM MO 1

MORIZONTAL AXIS

X IN CM

Figure 15. The histogram of beam spot on the SOS-HNSS target. The beam is defocused to 2.5x0.1 cm2 by the quadrupole cluster in the second match section.

Figure 16. The histogram of beam spot on the HMS target. The beam is achromatically transported by the quadrupole cluster in the second match section.

HALL C BEAM LINES 0.6 $dP/P=10^{-4}$ AMPLITUDE X IN CM $dx_0 = dy_0 = 0.01cm$ 0.4 $dx_0' = dy_0' = 0.01 mr$ 0.2 Target Arc lines AMPLITUDE Y 0.0 0.2 150 100 50 0 AXIAL DISTANCE Z IN METER

Figure 17. The beam envelope along Hall C beam line for beam energy measurement. The all sextupoles and beam correctors are switched off, therefore, the arc works as "spectrometer" mode.

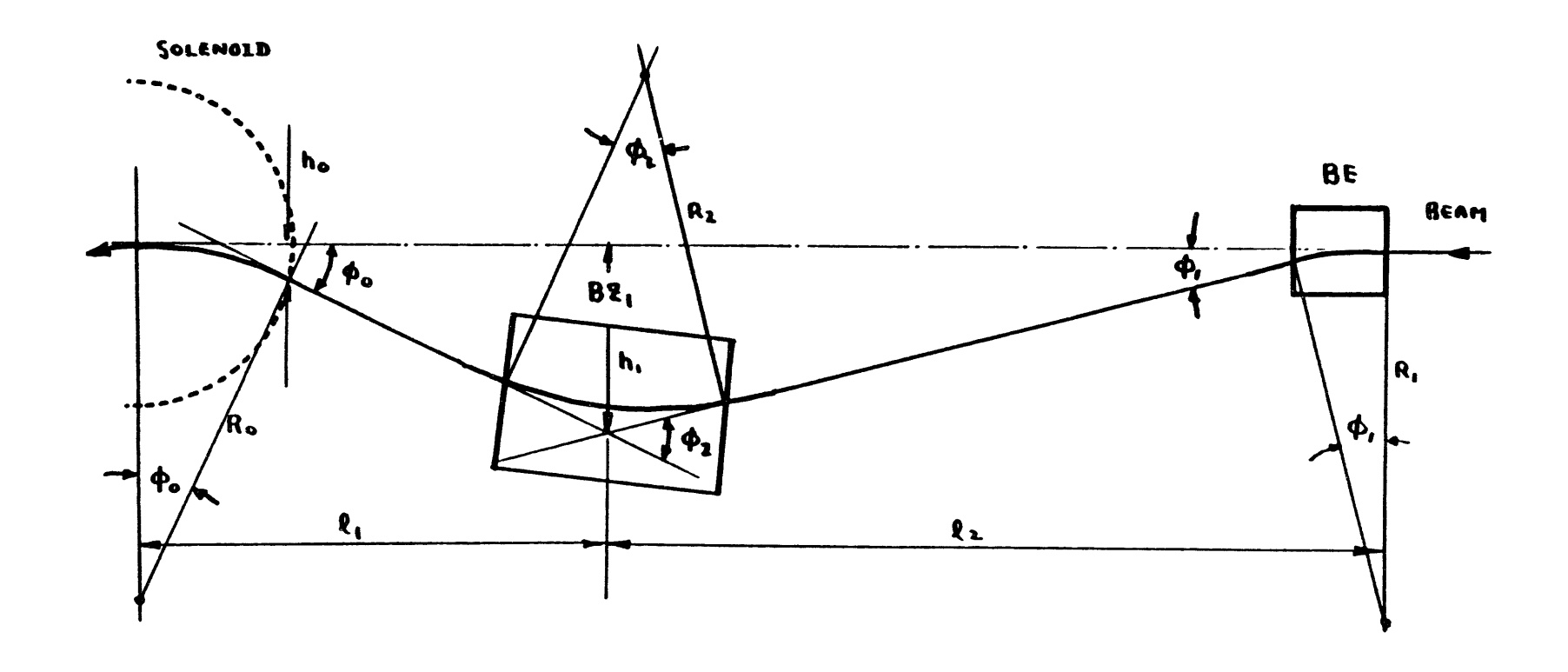


Figure 18. Layout of Hall C chicane system for UVa polaried target. The system is also used for compensation of Hall sink. After rotating 90 degree chicane will be used to transfer the beam to HNSS target which has 6 cm offset to the HMS target position.

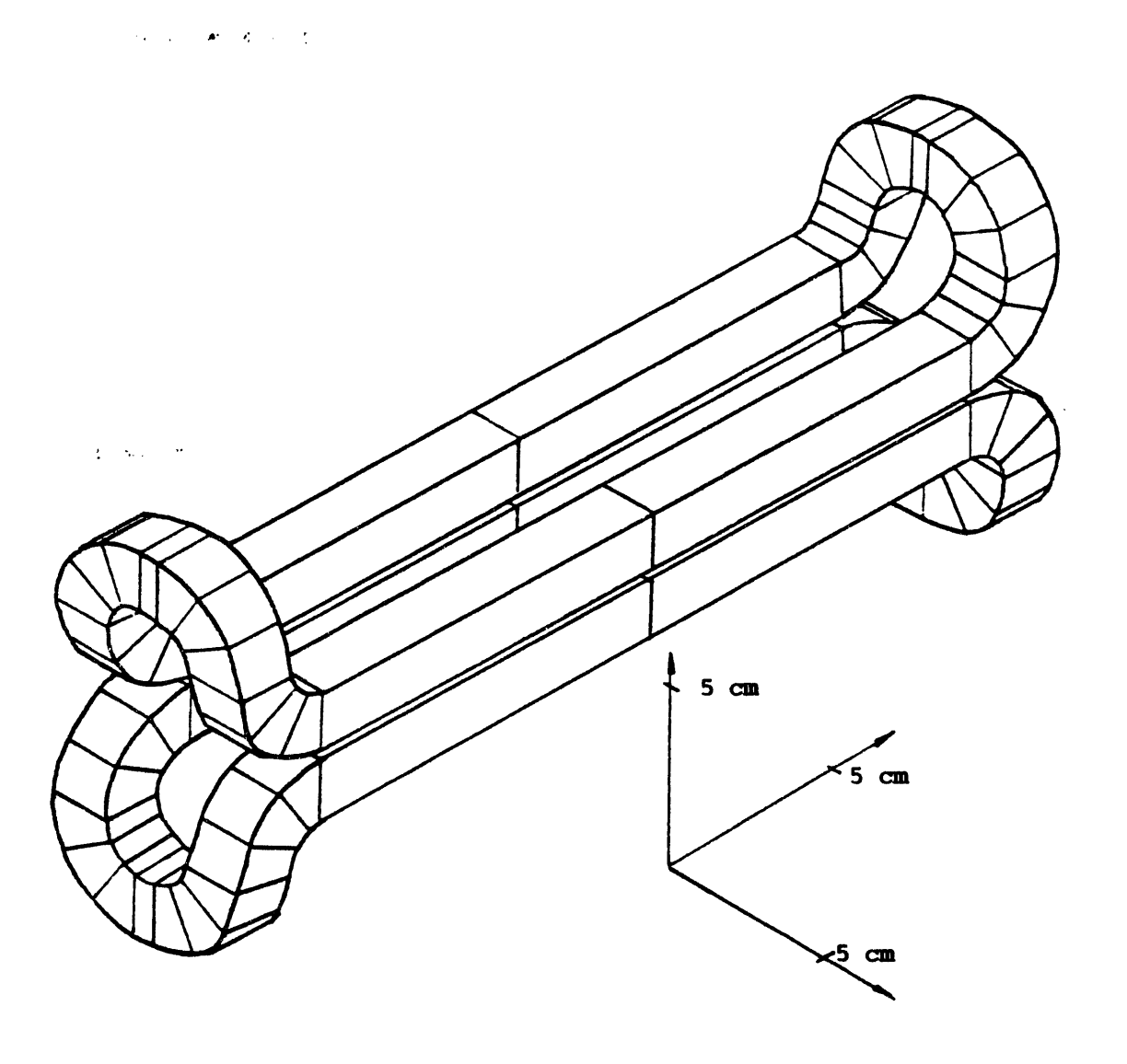


Figure 19. Fast raster geometry used in TOSCA calculations.

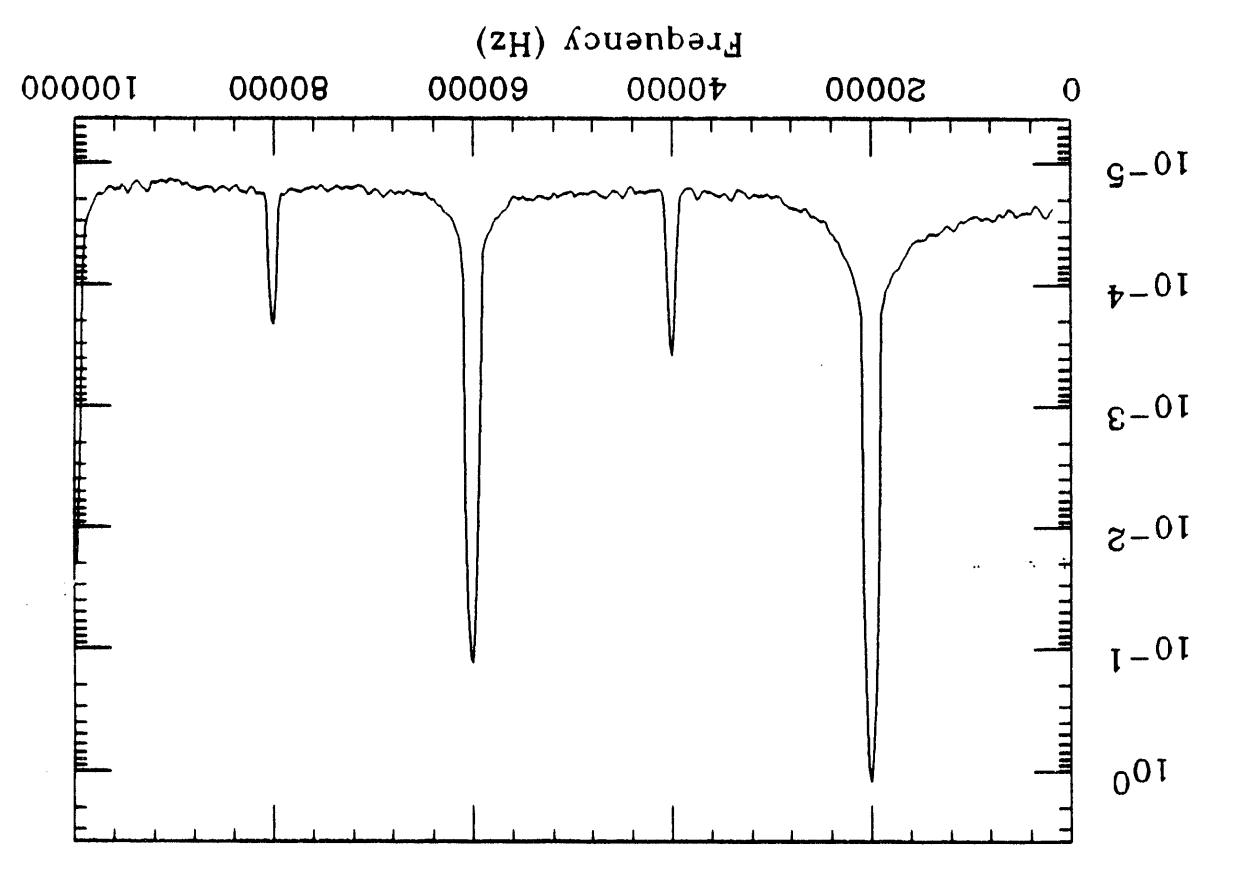


Figure 20. Frequency spectrum of triangle driving waveform and the main harmonic components are 3-rd (60 kHz) and 5-th (100 kHz).

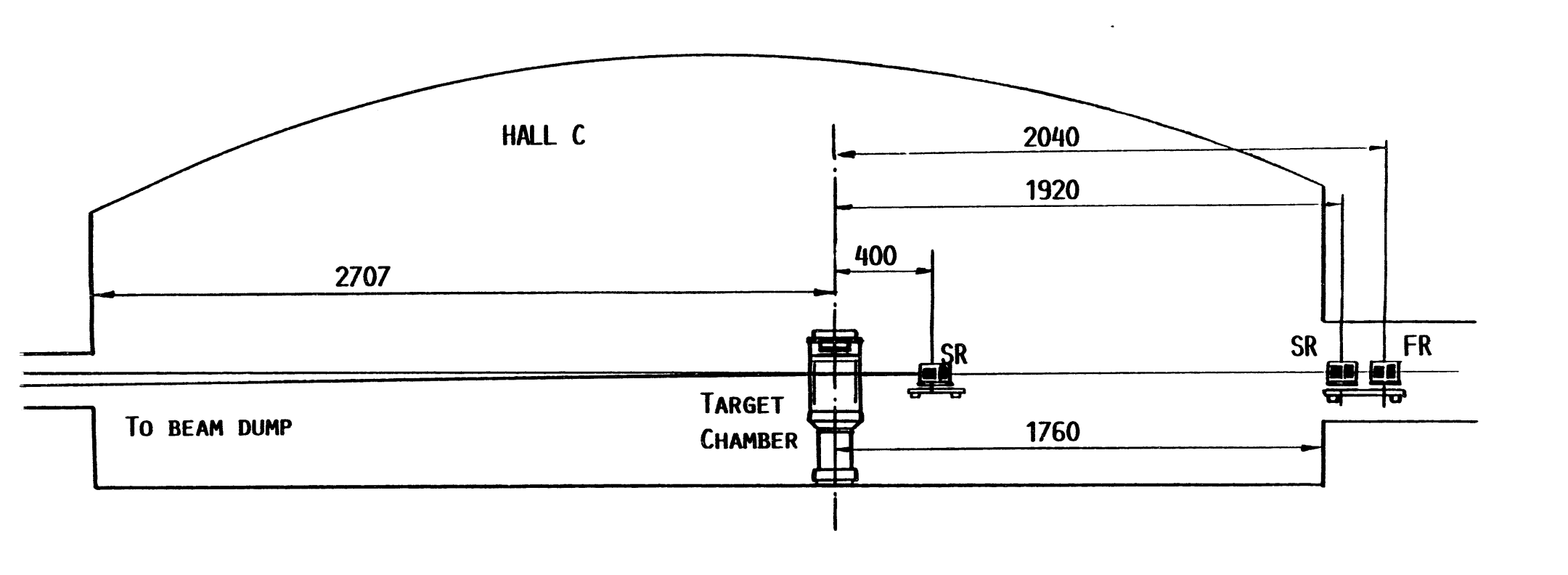


Figure 21. The raster system in Hall C. (FR = fast raster, SR = slow raster) The fast raster, located at the entrance of Hall C, provides 10 - 15 kHz rastering on HMS cryogenic target. Together with the first slow raster, this FR generates a composite rastering pattern on UVa polarized target. The second slow raster placed 4 m in front of the target provides 4x4 cm2 pattern on the beam dump.

